MICROSTRIP PATCH ANTENNA ARRAY FOR COVERAGE AND RANGE EXTENSION OF RFID APPLICATIONS

by

MEHMET ABBAK

Submitted to the Graduate School of Engineering and Natural Sciences

in partial fulfillment of

the requirements for the degree of

Master of Science

Sabanci University

August, 2008

MICROSTRIP PATCH ANTENNA ARRAY FOR COVERAGE AND RANGE EXTENSION OF RFID APPLICATIONS

APPROVED BY:

Assoc. Prof. İbrahim TEKİN …….

(Thesis Supervisor)

Assoc. Prof. Meric OZCAN …….

Assist. Prof. Güllü Kızıltaş ŞENDUR …….…….

Assist. Prof. Ayhan BOZKURT …….…….

Bahattin TÜRETKEN, PhD ……..…….

DATE OF APPROVAL: …….

MICROSTRIP PATCH ANTENNA ARRAY FOR COVERAGE AND RANGE EXTENSION OF RFID APPLICATIONS

Mehmet ABBAK

EECS, MS Thesis, 2008

Thesis Supervisor: Assoc. Prof. Dr. İbrahim Tekin

Keywords: Microstrip Patch Antenna, Antenna Array, Passive UHF RFID Systems

Transmission Line Phase Shifter, Wilkinson Power Divider, Range and Coverage

Extension

Abstract

Passive UHF RFID systems have various advantages over other RF based identification systems despite the lack of operation range and coverage as other passive systems, which is one of the main obstacles of this promising technology.

To increase the operation range and the coverage, in this thesis, phased antenna array for passive UHF RFID applications designed, implemented and measured. As a part of the phased antenna array design, a feed network, which will sustain the necessary amplitude to each radiating element and phase difference between them, is designed. This feed network design is composed of the separately design of phase shifter and power divider. Also as the radiating element, a microstrip patch antenna element is designed and implemented. After calculating the response final array structure with use of a phase shifter, power divider and microstrip patch antenna, to obtain beam steering between ±30 degrees, the antenna array is implemented on PTFE woven-glass ceramic composite substrate with a dielectric constant of 4.5.

From the radiation pattern measurements in the compact test range and experimental test results obtained in actual RFID system, it is observed that the operation range and coverage are increased. Also, it is acknowledged that compact test range and field tests of antenna array are consistent with each other. As a final remark, due to time averaging while steering between the main beams, without causing any issue with the ETSI regulation limits on ERP (effective radiated power), operation range and coverage can be expanded.

Mikroşerit Yama Dizi Anten ile Pasif UHF RFID Sistemlerinde Erim ve Kapsama Alanı Artırımı

Mehmet ABBAK

Elektronik Mühendisliği, Yüksek Lisans Tezi

Tez Jürisi: Doç. Dr. İbrahim Tekin (Tez danışmanı), Doç. Dr. Meriç Özcan, Yrd. Doç. Dr. Güllü Kızıltaş Şendur, Yrd. Doç. Dr. Ayhan Bozkurt, Dr. Bahattin Türetken

Anahtar Kelimeler: Mikroşerit Yama Anten, Dizi Anten, Pasif UHF RFID Sistemleri İletim Hattı Faz Kaydırıcı, Wilkinson Güç Bölücüsü, Mesafe ve Kapsama Arttırımı

Özet

Pasif UHF RFID sistemleri, operasyon mesafesi ve kapsama alanı bakımından diğer aktif RF tabanlı tanımlama sistemlerine göre eksik kalsa da, bu sistemlere göre farklı birçok avantajları bulunmaktadır. Operasyon mesafesi ve kapsama alanI limiti bu gelecek vadeden teknolojinin en önemli engel noktalarındandır.

Pasif UHF RFID sistemlerin operasyon mesafesini ve kapsama alanını arttırmak için bu tezde faz kaydırıcılı dizi anten tasarlanmış, gerçeklendirilmiş ve ölçülmüştür. Faz kaydırıcılı dizi anten tasarımının bir parçası olarak, her bir anten elamanına gerekli güç dağılımını ve faz farkını sağlayacak olan besleme devresi, tasarlanmıştır. Bu dizi anten besleme devresi tasarımı, faz kaydırıcı ve Wilkinson güç bölücülerin ayrı olarak tasarımından oluşmaktadır. Ayrıca, dizi anten içinde ışıma elamanı olarak da mikroşerit yama antenler tasarlanmış ve gerçeklendirilmiştir. Güç bölücü, faz kaydırıcı, besleme devresi ve mikroşerit yama antenler dizi anteni oluşturarak, ışıma örüntüsünün ±30 derece kaydırılmasının elde edildiği benzetimlerden sonra, dizi anten dielektrik sabiti 4,5 olan PTFE cam ve seramik örülü birleşiğinin üzerine basılmıştır.

Yansımasız odada yapılan ışıma örüntüsü ölçümleri sonucunda ve standart gerçek bir RFID sistemin içerisinde yapılan okuma testleri sonuçlarının birbirleriyle uyuştuğu be benzetimlerde görülen ışıma örüntüsünün kaydırılmasının elde edildiği ve böylelikle operasyon mesafesi ve kapsama alanı arttırılabilindiği ölçülmüştür. Son önemli nokta olarak, elde edilmek istenen yönlendirilmiş huzmeler arasında zaman da ortalaması alındığında, ETSI tarafından konulan efektif ışıma gücü düzenlemelerine karşı soruna neden olmadan operasyon mesafesi ve kapsama alanı arttırılabilinmektedir.

ACKNOWLEDGEMENTS

First and foremost I would like to thank and express my deepest gratitude to my thesis supervisor Assoc. Prof. İbrahim Tekin for his guidance, support, continuous encouragement and for keeping me motivated all the time. It was a great honor for me to have the chance to work with him for two years. I certainly could not come this far without his assistance. Moreover, I appreciate his patience and encouragement during the long laboratory hours.

I would also like to thank my dissertation members, Asst. Prof. Güllü Kızıltaş Şendur, Assoc. Prof. Meriç. Özcan, Asst. Prof. Ayhan Bozkurt and Dr. Bahattin Türetmen, for spending their invaluable time to review my thesis.

I would like to thank Dr. Nazli Candan and Dr. Bahattin Turetken of their assistance during the antenna / array measurements performed in the TUBITAK UEKAE Labs.

I would like to thank Turkish Scientific and Technology Research Institution TUBITAK supporting this project by Grant 104 E 123.

Last but not least, I would like to thank my family for their endless support in every step I take. With their unconditional love and moral support, I accomplished this dissertation.

Mehmet Abbak
2008

To my family…

TABLE OF CONTENTS

LIST OF FIGURES

1. Introduction

This thesis is aimed to design a microstrip patch antenna array operating at 867MHz for passive RFID systems. Main motivation behind the antenna array systems is to extending the coverage and operation range of the actual RFID systems. As part of the phased array system across a microstrip patch antenna is designed first as the radiating element. Further, power divider, phase shifter and feed network are designed and implemented to sustain essential beam steering.

An RFID system consists of tags, readers and an application host. The readers communicate wirelessly with the tags to obtain the information stored on them [1]. The data sent by the reader is modulated and backscattered from a number of tags. Many publications have studied RFID system design and its characteristics [2]. This communication principle is intended to operate in far field at UHF (ultra high frequency) range, on which this study is based on, and defined by ETSI for region 1 between frequencies 865.7MHz and 867.7MHz.

RFID applications are various and far reaching. Because there are so many numerous applications of RFID systems, there are different RFID systems working at different frequencies from KHz, MHz, to GHz range. They can be classified based on the power sources as passive, active and semi-active systems. In this thesis passive RFID system as defined by ETSI for region 1 between frequencies 865.7MHz and 867.7MHz is used. Major advantages of passive RFID systems are the low cost of the tags, and also, easy manufacturability, however, they have limited coverage and operation range. *Thus, the main objective of the thesis is extending the coverage area and operation range of passive UHF RFID systems*. The coverage and the operation range of a passive system can be increased by increasing the

transmitted power; however it is not feasible due to regulations on EIRP (effective isotropic radiated power).

So, by using the same transmit power operation range of the communication channel can be increased. In our approach, one of the antennas of the bi-static reader will be replaced by the phased antenna array, with a more directive beam with higher gain. The operating range of a RFID system is based on tag parameters, such as tag antenna gain and radar cross section, distances between readers, operating frequency, transmission power from reader to the tag, and gain of the reader antenna. Evaluating these parameters different approaches to increase the operation range and coverage of a RFID system can be obtained. Different ways of increasing the range of UHF passive RFID systems have been discussed in the literature. Increasing the sensitivity of RFID reader which can work with weaker signals received from tag, reducing power consumption, and increasing power efficiency on the tag circuit can be one way of increasing the operation range [3]. Other improvement suggestions when designing the RFID tag antenna and chip concurrently to decrease turn-on voltage of the tag chip for increased reading range operation is given in [4]. Furthermore, a theory of diversity system that could decrease the required power level for the same bit error rate, and therefore increasing operation range, is investigated in [5]. In addition, the operation range of the hand-held RFID reader for different types of patch antennas has been investigated and, shows that gain of the antenna is a fundamental factor of RFID system range in [6]. However, most applicable way of increasing the read range of UHF RFID system is increasing the gain of the reader antenna since there is a relaxed size limitation, unlike that of the RFID tag.

The thesis is organized as follows;

Chapter 1: This chapter provides the introduction to the thesis, objective and scope of work.

Chapter 2: Gives essential background about passive back-scattering RFID systems and covers the literature review on microstrip antennas, and final design stage of microstrip patch antenna element is investigated

Chapter 3: Analyzes the elements of feed network of the microstrip antenna array, like power dividers and phase shifter.

Chapter 4: Antenna array analysis and design of feed network is analyzed. Also, results obtained from simulations and measurements of antenna array are given. Also, test results of the antenna in the actual RFID systems are presented.

Chapter 5: Conclusion and possible future work for this thesis is given.

2. Background

2.1 RFID System

The read range or operation range of a passive tag is limited by its ability to provide sufficient voltage and power at the antenna to power the tag's integrated circuit. To extend the range of an UHF passive RFID system, in a basic sense, received power should be increased. Based on Friis transmission equation (Eqn.2.1), received power is based on the transmitted power, wavelength, distance, and gains of the antennas on both TX and RX sides.

$$P_R = P_T \left(\frac{\lambda}{4\pi R} \right)^2 G_{0t} G_{0r} \tag{2.1}$$

where $(\lambda / 4\pi R)^2$ is called the free space loss factor, wavelength λ and distance R are variables within this factor and, are constant for each application. Also, max transmitted power P_T is limited according to regulations on UHF RFID systems. Other remaining factors are the gains of the antennas of the reader and tag. In based on the mono-static approach, two antennas are used on the reader side where, one transmits and other receives signals. When the reader has two antennas, for receiving and transmitting purposes, respectively , we can conceptualize the unit as a radar system, due to transmission from tag to the reader, backward communication link is purely scattering in UHF RFID systems. This modal can be represented as in the Figure 2-1, where a passive backscatter RFID system model is given. Radar cross section, σ, a measure of an object's ability to reflect electromagnetic waves, is added to illustrate the power scattering function of RFID tags.

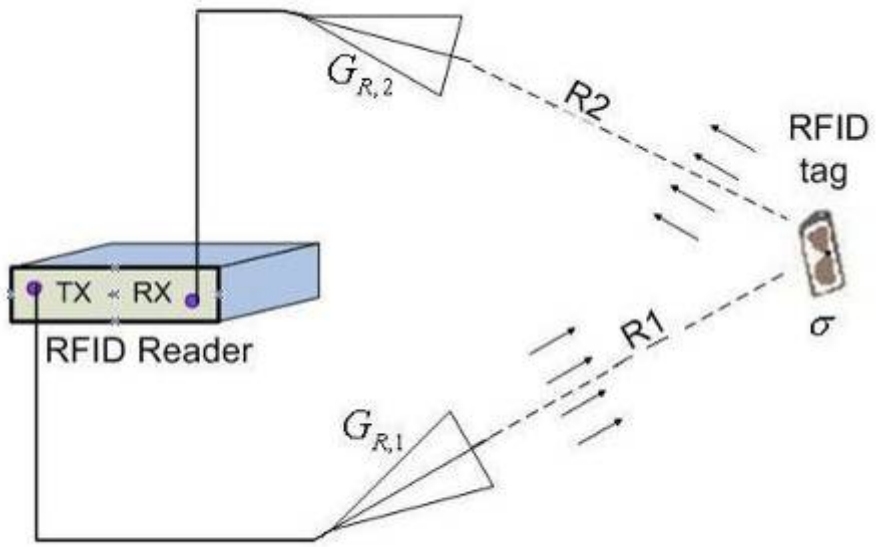

Figure 2-1: Bi-static RFID System

In the light of this model, we can construct a general formula for received power, which will mainly affect the operation range of a wireless system. Received power at the receiver reader in Figure 2-1, can be written as in Eqn.2.2.

$$P_R = \frac{P_T G_1 G_2 \sigma}{R_1^{\,2} R_2^{\,2}} \left(\frac{\lambda}{4\pi} \right)^4 \qquad (2.2)$$

For the maximum possible operation range, a minimum received signal level is specified. In other words, there is a minimum P_R for which the system is operable. For a fixed $P_{R,Min}$, to increase the range of RFID operation, R_1 and/or R_2, either receiver and transmitter antenna gains G_1 or G_2 can be increased.

The number of receiving and transmitting antennas is another factor affecting the operation range of the system. New approach on the RFID systems is multi-static system design due to its significantly better sensitivity to weak tag backscatter signals and superior RF coverage area. To demonstrate the advantage of this approach, in which two antennas can both receive and transmit, radiated power level contours are plotted. For a certain signal level, bi-static approach offers larger coverage as shown in Figure 2-2. As it is seen in Figure 2-2 , mono-static system that has one node that receives and transmits concurrently has less coverage for a certain level of signal compared to a system with multi nodes. By this method, coverage of a passive RFID system is increased by using multiple transmit and receive nodes, however, operation range can not be increased in terms of the distance of the tag with reference to the nearest antenna.

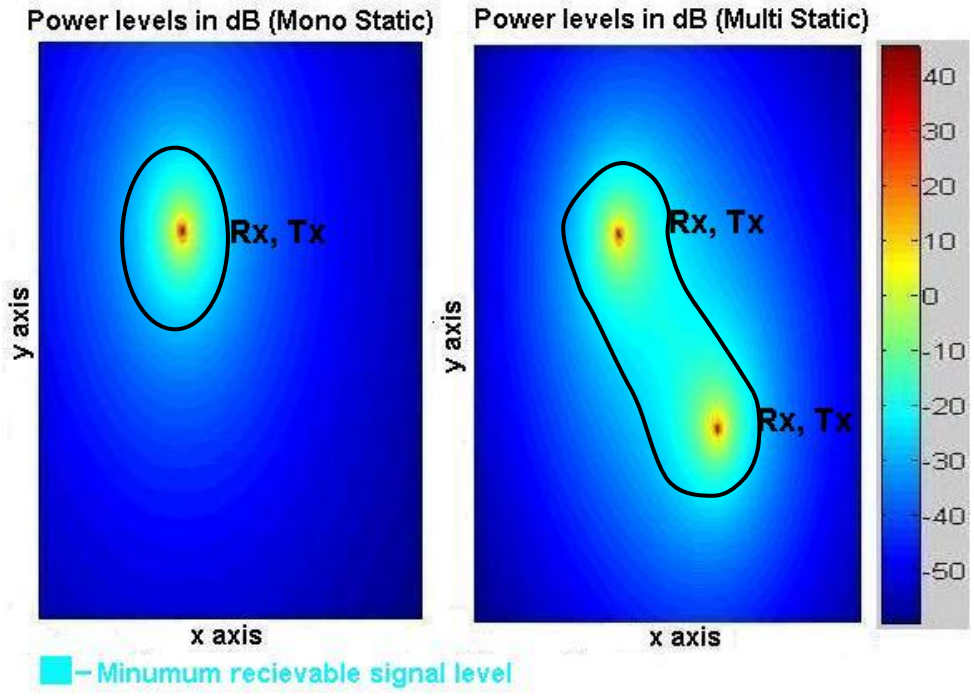

Figure 2-2: Mono-Static vs. Bi-static reader coverage

2.2 Basic Antenna Parameters

The performance and evaluation of the antennas are determined by several factors as follows;

2.2.1 Reflection Coefficient (Γ) and Return Loss (RL)

Transmission lines have a resistance related with it, which is called characteristics impedance, Z_0. however when the transmission line is terminated with an arbitrary load ZL, which is not exactly equal to its characteristic impedance, a reflected wave occur. And, reflection coefficient is defined to give the ratio between this reflected wave and the incident wave. It is derived by $\Gamma = \frac{Z_L - Z_0}{Z_L - Z_0}$. Return loss is the parameter that shows the amount of power that is reflected due to the impedance mismatch between the source and the load. And it is given by, RL = -20log | Γ| (dB).

2.2.2 Gain and Directivity

The gain of the antenna is the measure of the concentrating power in a certain angular region of space. The directivity of an antenna is defined as the ratio of the radiation intensity in a given direction from the antenna to the radiation intensity averaged over all directions. And relation between directivity and gain is defined by efficiency as G=ηD.

2.2.3 3dB Beamwidth

After the antenna pattern is plotted, some numerical aspects of the antenna pattern properties can be defined. And, half-power or 3dB beamwidth is the simply the measure of the angular width of the -3dB points on the antenna patter pattern relative to maximum level.

2.2.4 Bandwidth

The term bandwidth simply defines the frequency range over which antenna meets certain performance criteria. And it is generally defined through the return loss of the antenna, for the frequency band in which return loss is less than -10dB.

2.3 Microstrip Antennas

The concept of microstrip antennas was firstly presented by Deschamps as early as 1953 [7]. However, the first practical microstrip antenna was designed by Howell and Munson in the early 1970's [8], [9]. In particular, two techniques of feeding a microstrip patch were developed, the edge-fed patch and probe-fed patch, which are the ancestors of all other future developments [9]. Since then, widespread research has been committed to the study and further development of the concept of microstrip antennas. Use of patches in arrays was further investigated in the 1980's and microstrip phase antenna arrays were developed and analyzed [10]. The effects of the feed network on large arrays and achievable ultimate limitations on the overall size of a microstrip patch antenna array were investigated later [11]. Investigations into the microstrip patch antenna continued including radiation properties, in terms of means of efficiently producing circular polarization and other types of polarization [12], [13]. Microstrip antennas have many advantages such as light weight, low volume, low profile, low cost and compatibility with integrated circuits; hence the advantages of microstrip antennas make them popular in many applications that have need of a low profile and light weight antenna. Some of these applications are mobile radio, satellite communications, radars, biomedical radiators and reflector feeds. They can be made very thin and straightforwardly mounted on missiles, rockets and satellites. However, microstrip antennas also have some disadvantages compared to conventional microwave antennas such as narrow bandwidth, high loss, limitations on the maximum gain and lower power handling capability [14]. Microstrip patch

antennas come in many different shapes such as rectangular, square, circular and ring configuration. The rectangular patch is the most commonly used microstrip antenna. It is characterized by its length and width. The far field radiation pattern, resonance frequency, input impedance and bandwidth of rectangular microstrip patch antennas are well documented and reported in [15], [16]. Microstrip patch antenna is a simply kind of open wave guiding structure, which consists of a radiating patch on one side of a dielectric substrate and a ground plane on the other side [14]. Figure 2-3 shows a microstrip antenna in its simplest form. The radiating patch, usually made of copper, can have any form, rectangular, square, circular, ring, elliptical, triangular or any other shape.

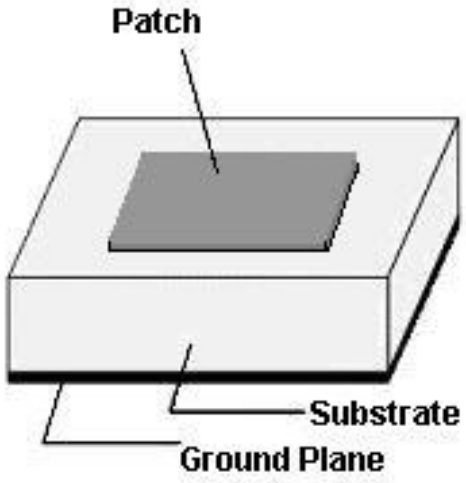

Figure 2-3: Microstrip Antenna Configuration

2.4 Rectangular Microstrip Patch Antenna

Rectangular shape is the most common patch shape because of its favorable radiation characteristics with low cross-polarization and ease of analysis and fabrication. The first and probably the most utilized patch conductor geometry

are the rectangular and square shapes. Linear and circular polarizations can be achieved with either single elements or arrays of rectangular microstrip patch antennas [14]. In general, the length of the patch controls the resonant frequency and the width of the patch affects the impedance level at resonance as well as the bandwidth; the larger the width of the patch, the smaller the input impedance of the antenna, and this statement is only valid under certain conditions, such as when the thickness of the substrate is greater than 0.03 λ_0, and in the design as a height of the substrate 0.0045 λ_0 is used. These relationships are not mutually exclusive and the feeding procedure and location can dramatically change all the measures of performance. This chapter covers the background theory of rectangular microstrip patch antennas and the reasons for chousing microstrip antennas as a part of the designed RFID system studied in this thesis.

It is fair to say that, for many practical designs, the advantages of microstrip antennas far outweigh their disadvantages. Microstrip antennas have been used in the frequency range from 100 MHz. to 100 GHz. Microstrip antennas, discussed in [14], have the following advantages:

- Light weight, low volume and conformal to surfaces of some vehicles,
- Low fabrication cost, so these antennas can be manufactured in large quantities,
- Both polarizations are possible
- Microstrip antennas can be easily integrated with microwave integrated circuits (MICs).
- Microstrip antennas are capable of dual and triple frequency operations.
- They can be manufactured mechanically robust when mounted on rigid surfaces.

Beyond these advantages, microstrip antennas have a number of disadvantages as compared to conventional antennas. The major disadvantages, discussed in [14], are given below:

- Narrow bandwidth (this can be increased by using thicker substrate, etc.),
- Low transmitting power, up to about 100 W.
- Most of them radiate into the half space,
- Surface wave excitation decrease the efficiency,
- Cross polarization

In this section, it is tried to answer why microstrip antennas are so popular in many antenna applications. There are vast amount of inexpensive opportunities for giving the circuit shape on a substrate material and producing the related mechanical mounts. The following work will only be the soldering, mounting and testing processes that most of the time one could easily handle by itself. Microstrip antennas have some disadvantages as explained before, but they will not be very critical when designed with some special techniques and dealt with adequate sensitivity. Due to the increasing demand for these antennas, many efforts have been made to reduce their disadvantages. To analyze one by one of these drawbacks given above, the narrow bandwidth of the microstrip antenna is a major obstacle for using it in today's communication systems. The operating range of the basic microstrip antenna element on a thin substrate is generally limited by its narrow impedance bandwidth. Bandwidth of microstrip antenna increases monotonically with thickness, but the problem with using a substrate thicker than the above range is that the impedance locus of the element becomes increasingly inductive [26], [27], making impedance matching increasingly difficult. In the applications that do not need much bandwidth like RFID, it turns out to be an advantage, to have narrow bandwidth, because the antenna rejects the signals that are out of the band and quality factor

increases. Also, for wireless communication systems like RFID there are power limits, so, lower transmitter power is not an issue for communication systems. Moreover, in the antenna array system natural half-space radiation pattern will be much more directive. Furthermore, by use of low loss and thin ($h<0.1\lambda_g$) microwave laminates, the effect of surface wave excitation will be decreased.

2.4 Method of Analysis

All the antenna designs in this thesis are analyzed using the well-known electromagnetic analysis method called Method of Moments (MOM). This technique transforms the integral equations into a matrix algebraic equation that can be easily solved by a computer In the MOM, the surface currents are used to model the conducting microstrip patch elements whereas the effects of dielectric layers of infinite-extent are taken into account by using the Green's functions. For the case of finite size dielectric layers, volume polarization currents in the dielectric slab are used to model the fields in the dielectric slab. An integral equation is then formulated for the unknown currents on the microstrip patches and the corresponding feed lines [17]. The integral equations are transformed into algebraic equations that can be easily solved using a computer. This method takes into account the fringing fields outside the physical boundary of the two-dimensional patch, thus providing a more exact solution. For a comprehensive list of references on this method, please refer to [18]. This thesis makes extensive use of commercially available software code ADS Momentum 2.5 D electromagnetic simulation tools [19] based on MOM to design and analyze all the configurations addressed herein.

2.5 Microstrip Antenna Feeding Techniques

Microstrip patch antennas can be fed by a variety of methods. These methods can be classified into two categories- contacting and non-contacting. In the contacting method, the RF power is fed directly to the radiating patch using a

connecting element such as a microstrip line. In the non-contacting scheme, electromagnetic field coupling is done to transfer power between the microstrip line and the radiating patch.

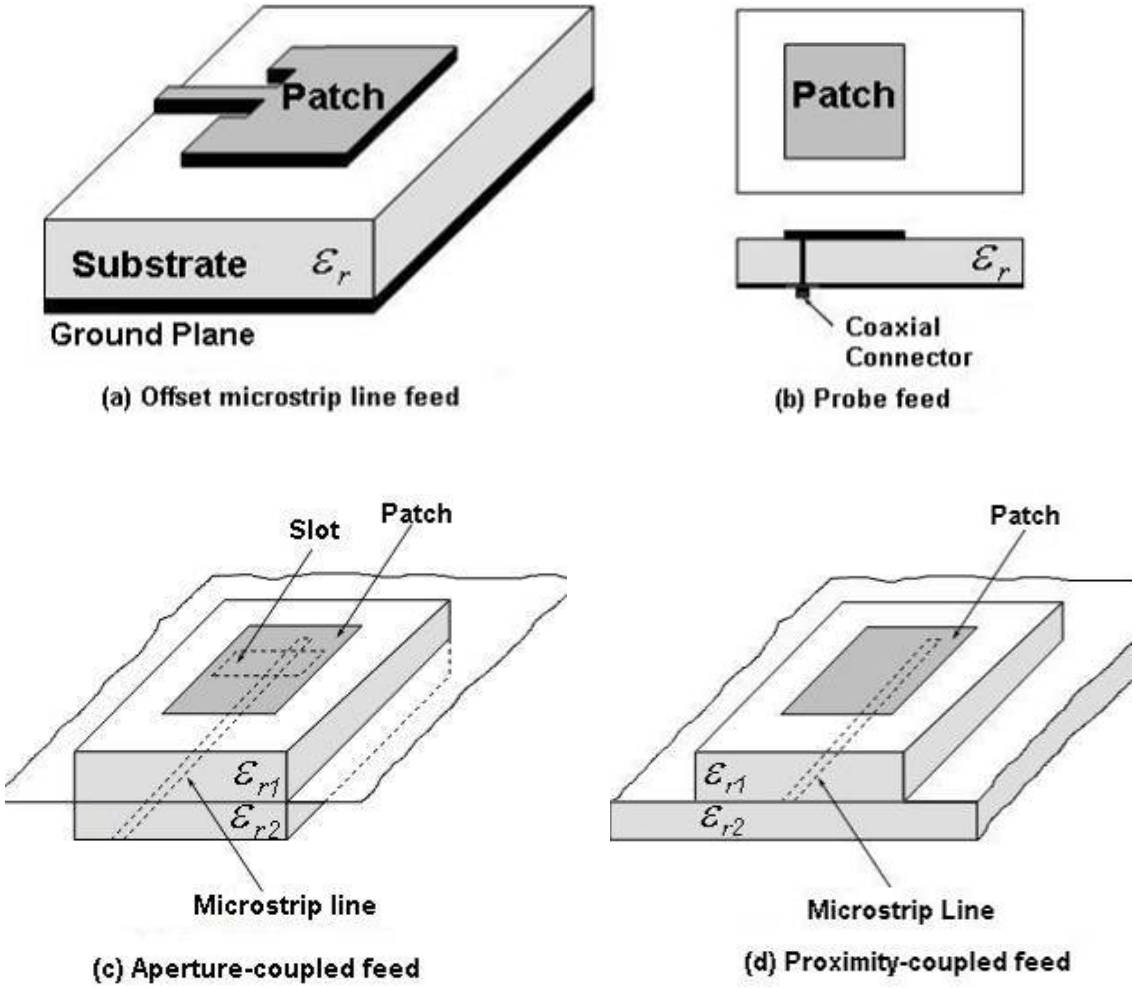

Figure 2-4: Feed configurations for microstrip antennas [21]

The coaxial feed tends to have a narrow bandwidth and is difficult to model analytically. The aperture-coupled feed isolates the feed mechanism from the radiating element through the use of a ground plane. Energy from the feed line is coupled to the element patch through the aperture slot. Unfortunately, the ground plane makes this feed configuration quite difficult to manufacture. Finally, the proximity-coupled feed removes the ground plane so it is easier to manufacture than the aperture-coupled feed [21]. Inset microstrip line feeding is

used for each microstrip patch antenna element as the most effective reasonable way to construct the antenna array, due to its planar structure and, it eases the task of matching since inset depth controls the input impedance of the antenna. Additionally, this configuration is simple to fabricate and lends itself well to analytical modeling.

2.6 Microstrip Patch Antenna Design

Various analysis techniques exist for modeling microstrip antennas [20] and the three most popular techniques used are the transmission-line, cavity and full-wave models [21]. The transmission-line model is the simplest to implement, and cavity model, which has better accuracy but increased complexity, are empirical models that utilize assumptions to simplify the computation. The full-wave model entails an exact analysis of Maxwell's equations, which is computationally expensive, and potentially provides the best precision as it considers boundary-conditions on the dielectric-air periphery. Both the cavity and transmission-line models have the added advantage of providing the designer with a good physical perception and are computationally efficient. Equations based on the transmission line model, which models each edge of the rectangular patch as a thin radiating aperture [21], [22], are used as a guide in the initial phase of designing a patch antenna. CAD optimization is then usually used to tweak the antenna design to the desired performance or when evaluating various antenna substrates and dimensions.

2.6.1 Microstrip Patch Antenna Formulations

Microstrip patch antennas have been examined using assorted techniques. The transmission-line model is the simplest compared to cavity model and full wave numerical models, however, it is the least accurate. In designing a rectangular

patch microstrip antenna, the formulas that were derived are used as an outline in design procedures.

In the transmission-line model the radiation from microstrip patch antennas can be calculated from the equivalent magnetic current distributions around the edges of radiating patch. The magnetic current values can be obtained from the edge voltage (with respect to the ground plane) distributions. Thus, the problem of microstrip antenna analysis reduces to that of finding the edge voltage distributions, for a given excitation and for a specified mode of the resonance of the patch.

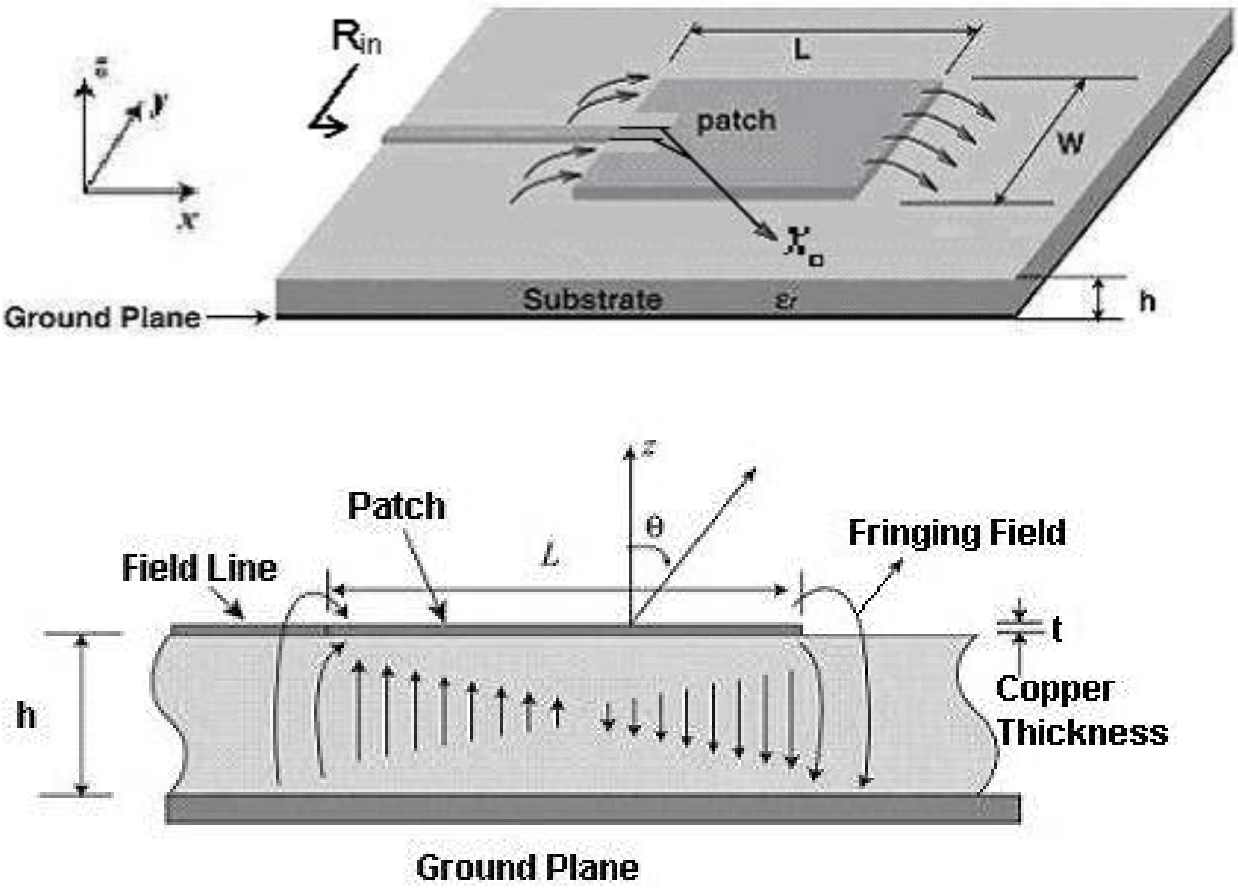

Figure 2-5: Transmission-line model of microstrip antenna

The microstrip antenna is modeled as two radiating slots that are separated by a distance L_{eff} . Referring to Figure 2-5, we can see the physical meaning of L_{eff} . It is essentially the length of the patch, L, plus an additional distance, $2\Delta L$, to account for the fact that electric field of an open microstrip line does not end suddenly and, the patch looks electrically larger than its physical dimensions due to the fringing fields. It can be either introducing a capacitance or equivalent length extension, and Balanis [21] compensated by the following formula for this additional length

$$\Delta L = 0.412h\frac{(\varepsilon_{reff}+0.3)(\frac{W}{h}+0.264)}{(\varepsilon_{reff}-0.258)(\frac{W}{h}+0.8)} \qquad (2.3)$$

In the above equation, ε_{reff} is the effective dielectric constant of a microstrip transmission line given by [15] whose value is determined by evaluating the capacitance of the whole fringing field. The value of ε_{reff} is slightly less than ε_r because the fringing fields around the periphery of the patch are not confined in the dielectric substrate but also spread in the air as shown in Figure 2-5.

$$\varepsilon_{reff} = \frac{\varepsilon_r+1}{2}+\frac{\varepsilon_r-1}{2}\left[1+12\frac{h}{W}\right]^{-\frac{1}{2}} \qquad (2.4)$$

In order to operate in the fundamental TM_{10} mode, the length of the patch must be slightly less than $\lambda_g/2$ where λ_g is the wavelength in the dielectric medium and is equal to $\lambda_0 / \sqrt{\varepsilon_{reff}}$ where λ_0 is the free space wavelength. The TM_{10}

mode implies that the field varies one λ/2 cycle along the length, and there is no variation along the width of the patch. For microstrip antennas the choice of the width of the patch, W, radiator is very important. Small values of W result in low antenna efficiencies while large W values lead to higher order modes [23]. Also, for efficient radiation the width W is given by Bahl and Bhartia [14] as;

$$W = \frac{c}{2 \times f_0 \times \sqrt{\frac{(\varepsilon_r + 1)}{2}}} \tag{2.5}$$

An expression for input impedance for microstrip patch antenna is given in [25] by using Cavity model analysis as

$$R_{in} = 90 \frac{e_e}{p c_1} \varepsilon_r \mu_r \left(\frac{L}{W} \right) \sin^2 \left(\frac{\pi x_f}{L} \right) \tag{2.6}$$

Where p is the proportion of patch antenna and Hertzian dipole in terms of radiated power,

$$p = 1 + a_2/20\ (kW)^2 + a_4(3/560)(kW)^4 + b_2(1/10)(kL)^2$$

And where $a_2 = -0.16605$, $a_4 = 0.00761$ and $b_2 = -0.09142$.

Also, c_1 in the Eqn. 2.6 is given as

$$c_1 = 1 - 1/n^2 + 0.4/n^4$$

Where n is the refractive index and equals $n = \sqrt{\varepsilon_r \mu_r}$. Also x_f is the probe position in the x-direction. Approximation holds for thin substrates and more accurate for substrates with low dielectric constant [25]

Inset fed can be approximated through experimental investigation [14] as, for inset fed length x_0 shown in the Figure 2-5, to match input impedance of the antenna R_{in}, necessary x_0 value can be obtained through eqn.2.6;

$$R_{in}(x = x_\circ) = R_{in}(x = 0)\cos^4(\frac{\pi}{w}x_\circ) \tag{2.6}$$

The rectangular microstrip patch antenna can be operated in several different modes. However, the most common modes of operation for the antenna are the TM10 and TM01 modes (Lo, at al, 1979) [15], Since they produce principal plane radiation patterns with maxima in the broadside direction. Higher order modes tend to produce maxima off broadside. If W is too large, then the higher order modes could get excited. The radiation pattern of rectangular microstrip antenna for the TM10 mode could be calculated by combining the radiation pattern of the two slots of length W and width ΔL on the infinite ground plane, which are spaced at a distance L + ΔL . Simple expressions exist which approximate the radiation patterns for the rectangular patch antenna and are given by [24]

$$E_\theta = E_0(\cos\phi)\, f(\theta,\phi) \tag{2.7}$$

$$E_\phi = -E_0(\cos\theta)(\sin\phi)\, f(\theta,\phi) \tag{2.8}$$

$$f(\theta,\phi) = \frac{\sin\left(\frac{\beta W \sin(\theta)\sin(\phi)}{2}\right)}{\frac{\beta W \sin(\theta)\sin(\phi)}{2}} \cos\left(\frac{\beta L \sin(\theta)\cos(\phi)}{2}\right) \tag{2.9}$$

Where first part of the Eqn. 2.9 is the pattern factor for a uniform line source with length W, and second part is corresponding to the array factor for two equally excited elements with spacing L. Further simplifications can be made to write the principal plane patterns as [24]

$$F_E(\theta) = \cos\left(\frac{\beta L \sin(\theta)}{2}\right) \tag{2.10}$$

$$F_H(\theta) = \cos(\theta) \frac{\sin(\frac{\beta W \sin(\theta)}{2})}{\frac{\beta W \sin(\theta)}{2}} \quad (2.11)$$

Where θ is angle measured from the broadside as shown in Figure 2-5. Explicitly in Figure 2-6 where E-planes and H-planes of the microstrip patch antenna with designated start point for pattern measurement is plotted.

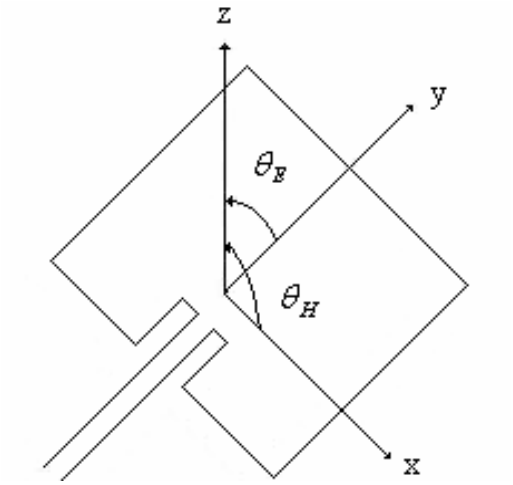

Figure 2-6: MPA (E-H plane)

2.6.2 Simulation

Upon completion of design and feeding method, in order to verify further the theoretical calculations, simulation is done using ADS Momentum software. ADS Momentum software is a full-wave electromagnetic simulator based on the method of moments (MOM) and is used to simulate the structure of the antenna. The antenna is drawn in the layout based on the designed dimensions. Layout is composed of two layers, one is patch layer and other one is ground layer. Feeding of patch layer is obtained through internal port and ground reference port to the internal port is defined at the ground layer.

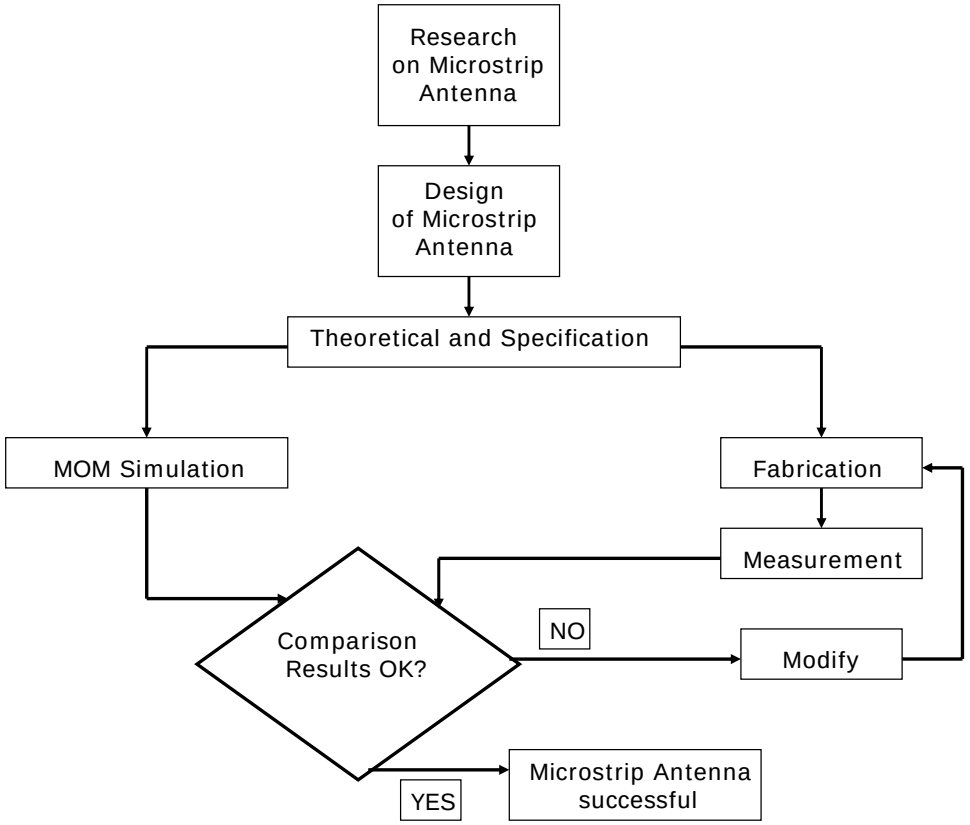

Figure 2-7: Design Methodology

Fabrication consists of three main stages. The stages are, UV exposure, developing and etching process. UV exposure is used to transfer the image of the circuit pattern with a film in a UV exposure machine onto to the photo resist laminated board. This process will usually take 2 minutes. To transfer the antenna on a film, Linkcad software is used. By using this software, the actual structure without any compression of the layout sizes of the simulated antenna can be transferred easily. In developing process, water added Sodium Hydroxide mixture removes away the exposed resist so that the pattern will be fully developed. In the final etching process, unwanted copper area on the PCB is removed by Ferric Chloride. After soldering the SMA connector to microstrip

antenna, it is available for measuring S-parameters in HP Agilent 8270ES 50MHz-20GHz S-Parameter Network Analyzer.

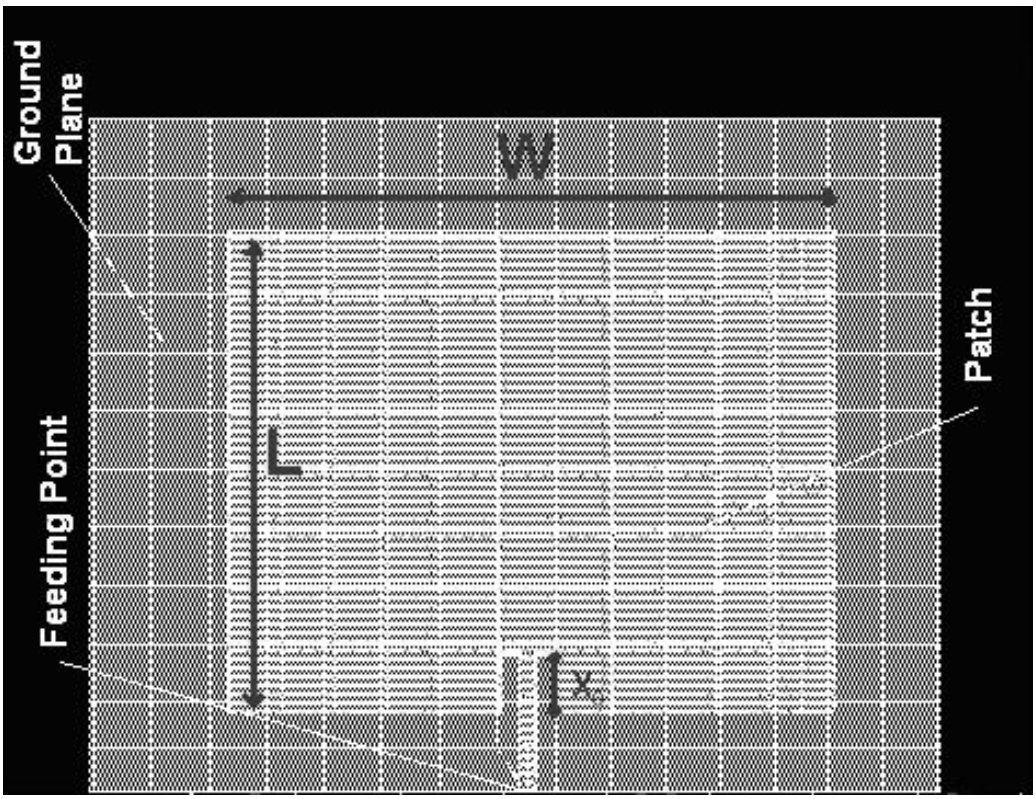

Figure 2-8: Layout model of the microstrip patch antenna

For parameters h=1.6mm and ε_r =4.5 using the theoretical initial values S-parameter simulations done in ADS Momentum. Geometrical values of for length of the antenna as L = 82.6mm, for width as W = 105.2mm and with a inset fed length x_0 = 29.6 mm. Return loss of the simulated microstrip patch antenna is plotted Figure 2-9. Antenna radiates at 867MHz with a return loss of -40dB.

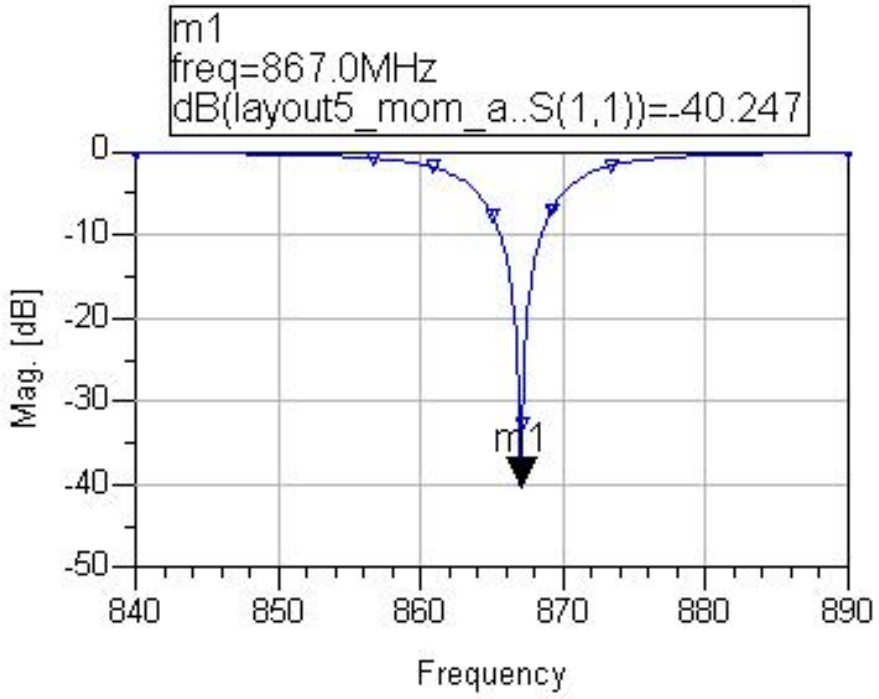

Figure 2-9: Simulation Results

To design a microstrip patch antenna which has very narrow bandwidth, design methodology explained in Figure 2-7 should be applied.

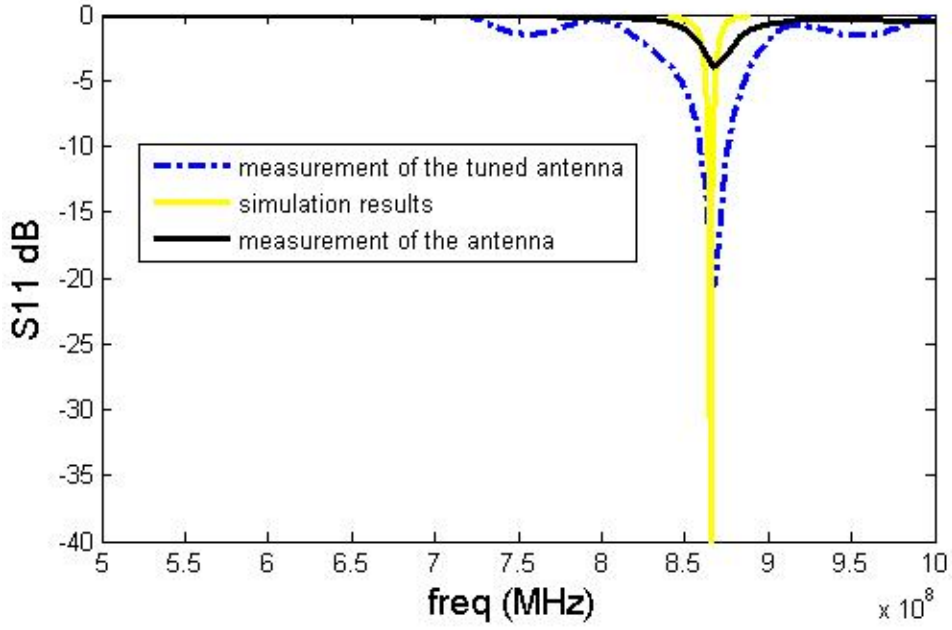

Figure 2-10: Design Methodology Example

To explain the steps while designing the microstrip antenna, Figure 2-10 is plotted. In this plot yellow line corresponds to the simulation result given in Figure 2-9, which has been derived by various simulations over the first initial geometry values obtained by formulas that are arise from transmission line model of microstrip antenna. Along with, black line shows the return loss of the measurement of the printed microstrip antenna with the given simulation in Figure 2-10, with design variables of Length=83mm and inset feed depth of 30mm. It is clear that there is apparent difference in terms of return loss and frequency between the simulated and actual measured antenna. Due to these differences between the measurement and simulation results additional microstrip antenna fabrication is needed. This process can be called tuning step. Fine tuning of the microstrip patch antenna is based on input impedance and resonance frequency. Fine tuning of the matching of the antenna is done through varying inset-fed length x_0 and this change in x_0 mainly does not affect the resonance frequency. To obtain necessity resonance frequency fine tuning can be done by changing the length of the rectangular patch, which is also will not affect the matching of the microstrip patch antenna. After various fabrication and measurements final version of the microstrip patch antenna is realized, and return loss of this antenna is plotted as blue dotted line. Explicitly, all the s-parameter measurements done on the Agilent 8270ES S-parameter Network Analyzer, shown as phase and magnitude of return loss in Figure 2-12 and Figure 2-13. Realized microstrip patch antenna is can be seen in Figure 2-11. Final design parameters of antenna are as Width=106.7mm, Length=83.8mm and inset fed length of x_0 = 11mm. From the s-parameter measurements it is ascertained that antenna is radiating at 867MHz and by easily looking at the phase of return loss, and at this frequency magnitude of the return loss of the antenna is -23dB which means 99.5% of power is transmitted. Also, it is seen that 10dB return loss bandwidth of the antenna is 16MHz, between 860MHz – 875MHz, which is fairly sufficient for RFID applications.

Figure 2-11: Microstrip Patch Antenna

2.7 Microstrip patch antenna measurements

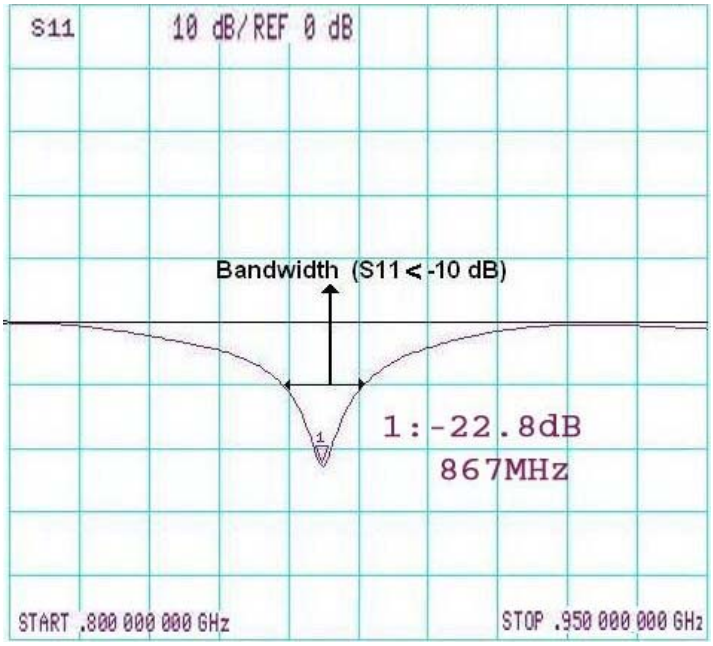

Figure 2-12: S11 (magnitude)

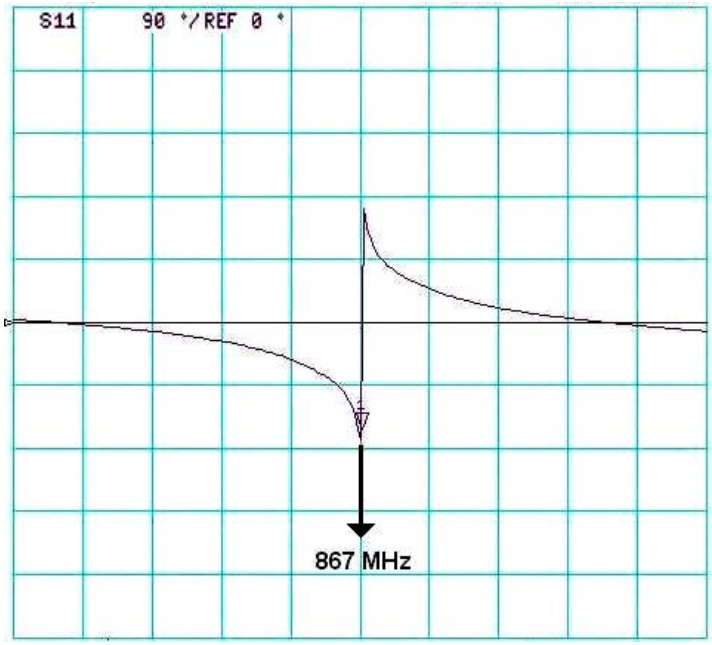

Figure 2-13: S11 (phase)

After completing S-parameter measurements, and understanding that microstrip patch antenna radiates at 867MHz, to understand the radiation characteristics of the antenna, it is measured in the compact test range facilities of the TUBITAK UEKAE labs. In the Figure 2-14 radiation pattern of co- polar and cross-polar of H-plane is plotted measured -3dB beamwidth in H-plane is 70.60 degree, and better than 15dB of co and cross polar difference is obtained at 867MHz. In the Figure 2-15 corresponding radiation pattern of E-plane for both co-polar and cross-polar is plotted. -3dB beamwidth of 80.78 degree is measured for E-plane and with a better than 15 of co and cross polar difference is measured. In the Figure 2-16, planar plot of the radiation patterns of E-plane and H-plane is given to ease understanding general structure of the patterns corresponding to cross-polar levels and angles with the help of the microstrip patch antenna Figure 2-6.

Becxause it is a planar antenna and has a major main lobe with minor lobes, to calculate the directivity of antenna, simpler equations such as Eqn.2.9 can be used. Using Eqn.2.9 approximated directivity is calculated as 7.22. If the

directivity of the antenna is calculated from Eqn.2.10 ratio of maximum and average radiation intensity, directivity is given as 7.66.

$$D \approx \frac{4\pi}{\theta_{hp}\phi_{hp}} \approx 7.22 \tag{2.9}$$

$$D \approx \frac{4\pi * U_{\max}}{P_{rad}} \approx 7.66 \tag{2.10}$$

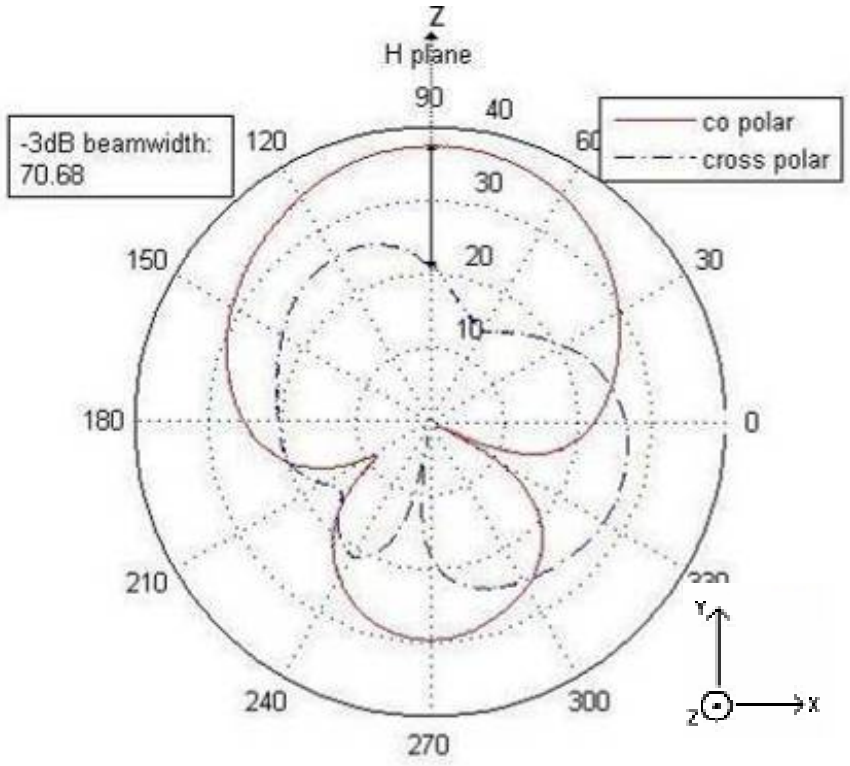

Figure 2-14: Measured co-cross polarization (H-plane) radiation pattern

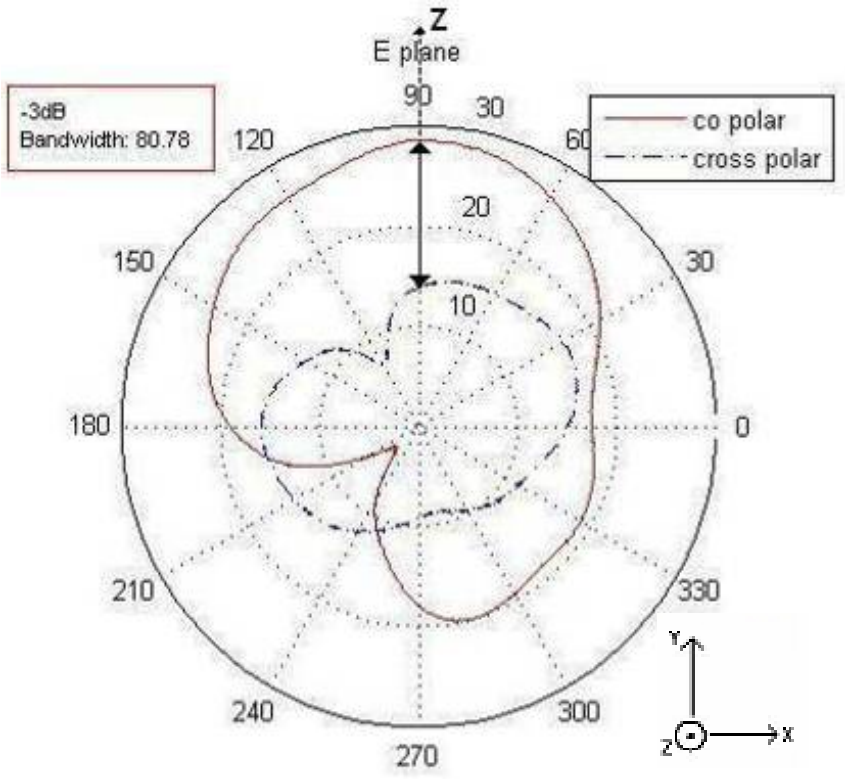

Figure 2-15: Measured co- cross-polarization (E-plane) radiation pattern

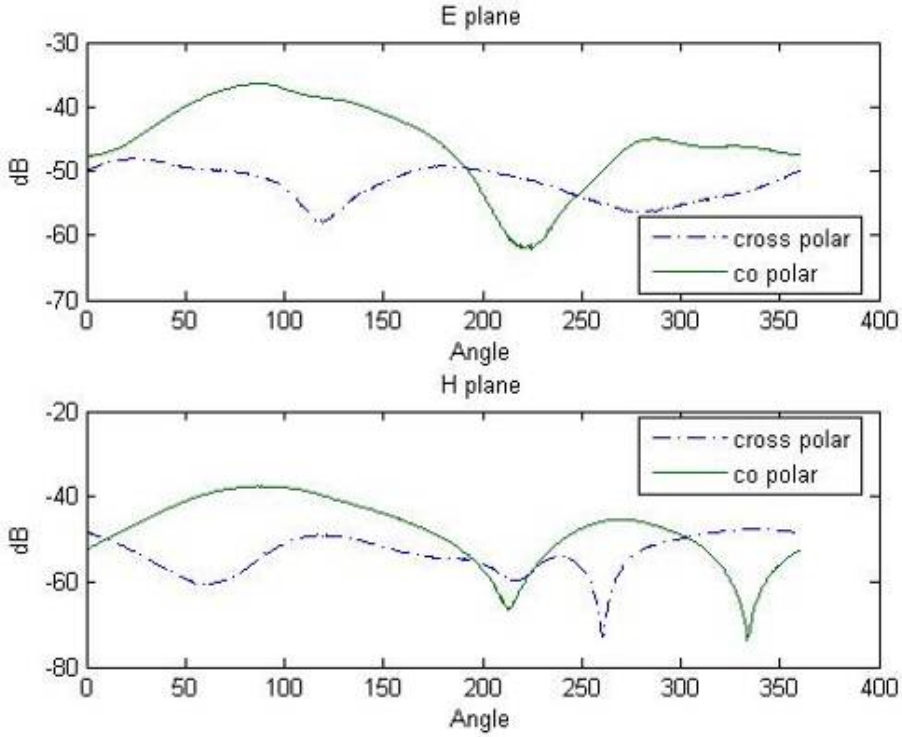

Figure 2-16: Radiation Pattern (Planar)

If you look at to the polar radiation pattern of the microstrip antenna, H-plane is more symmetrical and E-plane is not, which is caused by asymmetry due to feed structure, and inequality of width and length of the rectangular patch. At the boresight there is clear difference of co-cross polarization signal levels of this linearly polarized microstrip antenna. In the back lobe co cross polarization signal levels are much more close, and even for degrees cross polarization surpasses co polarization signal levels, due to refracted signals from the substrate mainly construct back lobe.

2.8 Radiation Pattern Measurement System

Compact test range measurements are done in the anechoic chamber of TUBITAK-UAKAE. The wall of the chamber is entirely enclosed with pyramidal microwave absorbers as shown as in the Figure 2-17. In the chamber, horn antenna must be replaced more far away $2D^2/\lambda$ than AUT (antenna under test) to be in the far field of the antenna, where D is the largest dimension of the antenna. Also, sweep time of the turn table to round 360° was set to 35sec. And in the Figure 2-18 microstrip patch antenna as an AUT is shown the compact test range.

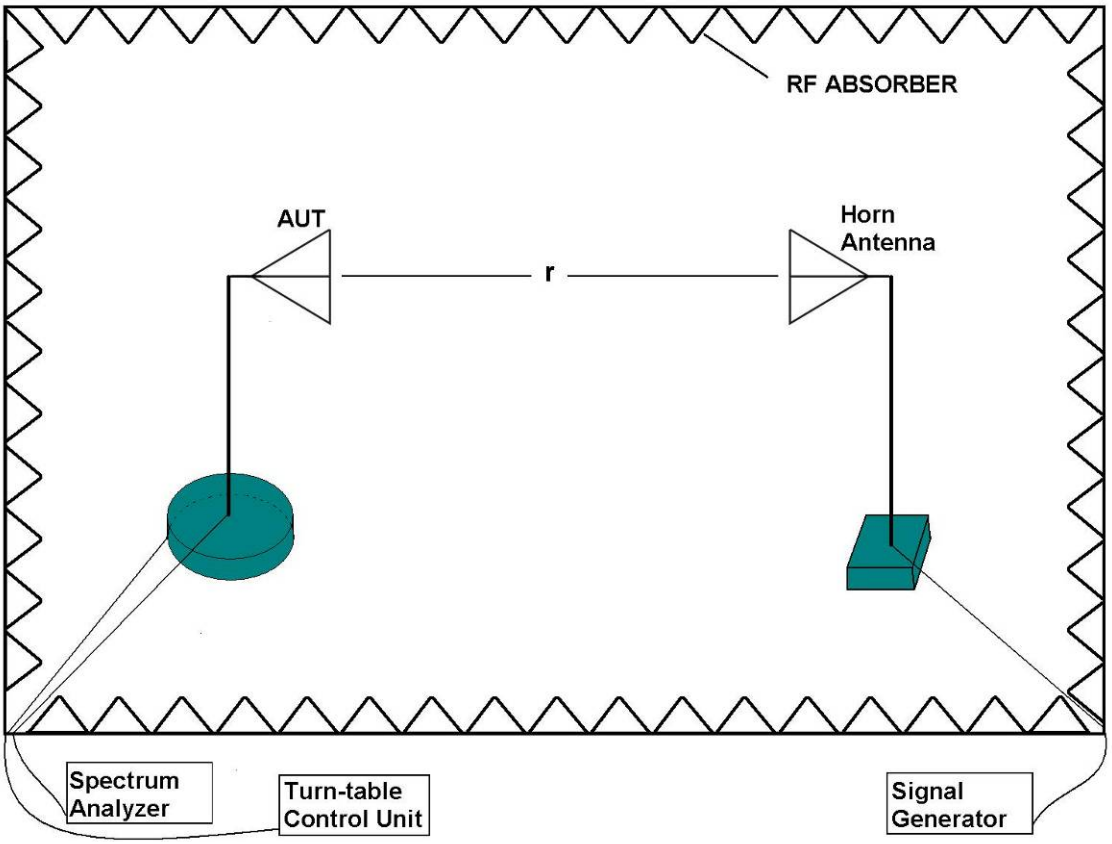

Figure 2-17: Compact Test Range

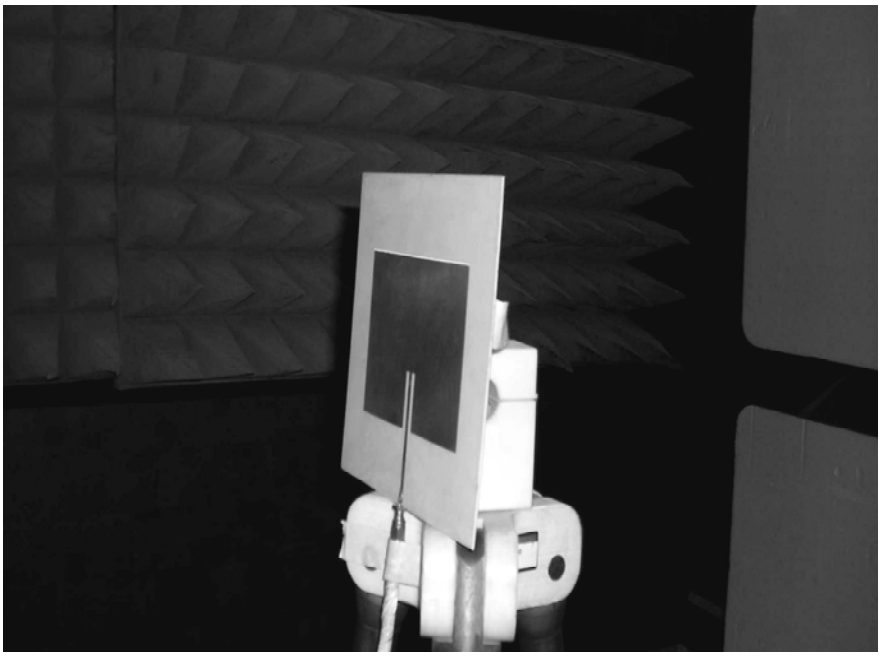

Figure 2-18: MPA in Compact Test Range

3. Microstrip Antenna Array Feeding Elements

In this chapter, phase shifter and power divider which form the antenna feeding elements will be explained in detail.

3.1 Phase Shifter

Phase shifters are used to vary the transmission phase angle of a feed network. Ideally, from phase shifters low insertion loss and equal amplitude in all phase states are expected. While, in various microwave applications they are used, in this thesis it will be used in phased array antenna system. General topology of transmission line phase shifter is given in Figure 3-1 .

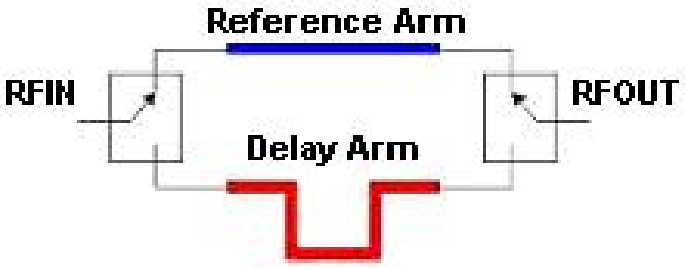

Figure 3-1: General Phase Shifter

Required phase shift can be provided by satisfying the equation $\Delta\phi = \beta(l_2 - l_1)$ using the difference between the delay arm and reference arm, where $\beta=2\pi/\lambda_g$. Phase shifter is printed on FR4 with dielectric constant $\varepsilon_r=4.5$. Also, because it is designed to be used in UHF RFID Antenna Array, electrical length is calculated according at f_0 = 867 MHz. For switching on two side of the phase shifter M/A-COM's single pole double throw (SPDT) switch with, 0.4dB insertion loss, is used.

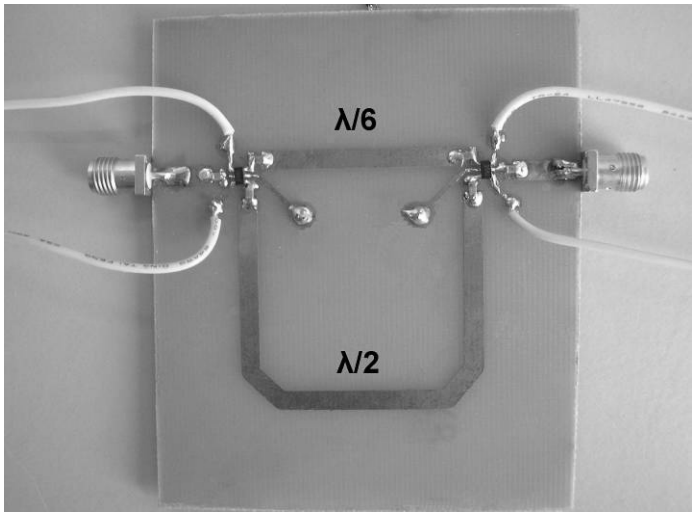

Figure 3-2: Phase Shifter

For the antenna array application, phase shifter with electrical length of λ/6 on reference arm and λ/2 on the delay arm was desired with difference of λ/3 to have ideal radiation pattern, so in the equation $\Delta\varphi=120/360*2\pi$. According to these, phase shifter is realized by PCB etching method as shown in Figure 3-2. Measurements are done with network analyzer with two ports. Measurements are divided in two; S-parameters of reference arm and delay arm are investigated.

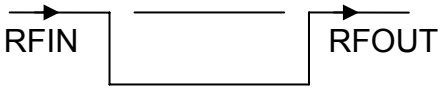

Delay Arm

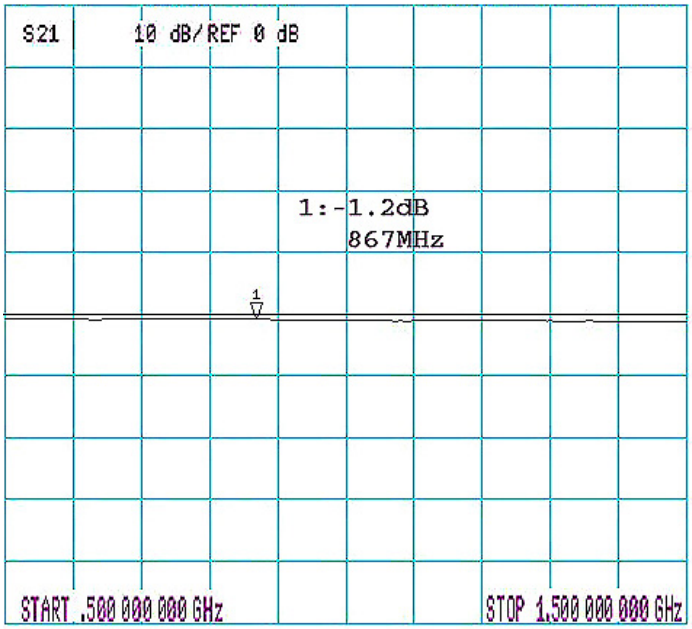

Figure 3.3: S12 (dB)

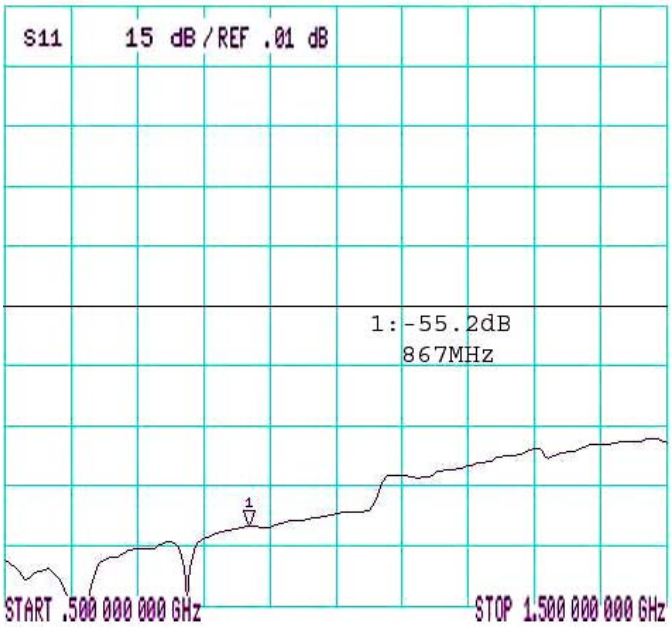

Figure 3.4: S11 (dB)

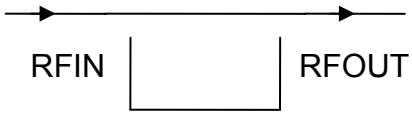

Reference Arm

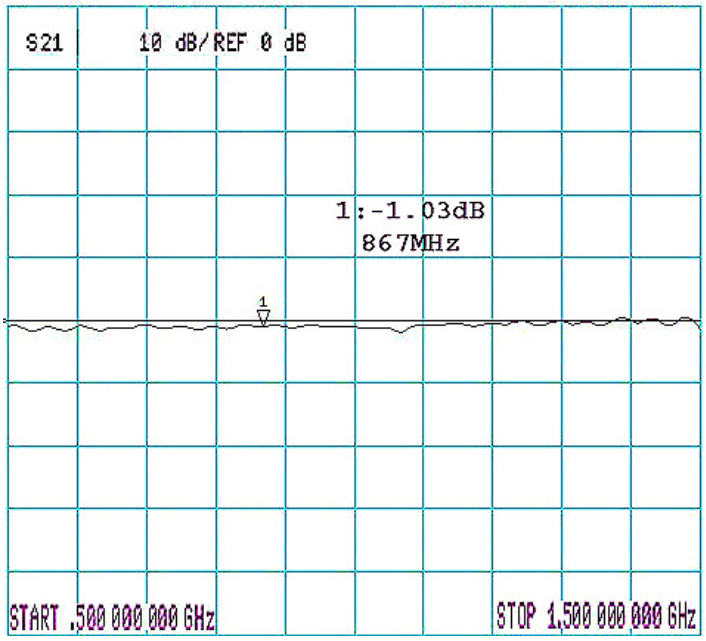

Figure 3.5: S12 (dB)

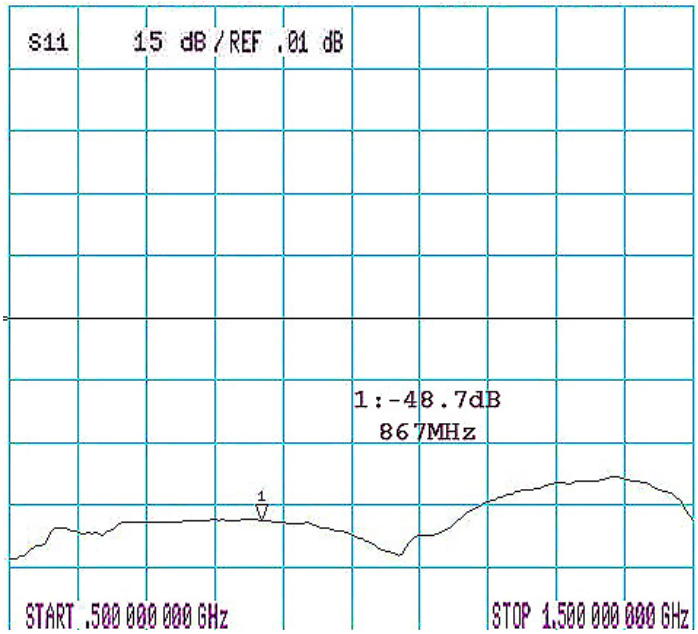

Figure 3.6: S11 (dB)

Results shows that phase shifter has low transmission loss both on delay and reference arm, which have a return loss of -1 dB and -1.2 dB respectively, and also has low reflection both on delay and reference arm that are -55.2 dB and -48.7 dB correspondingly.

Phases

Reference Arm

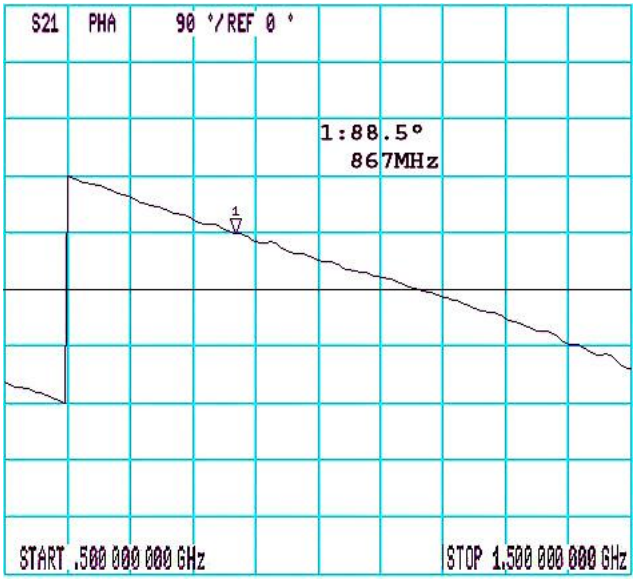

Figure 3.7: S12 (phase)

Delay Arm

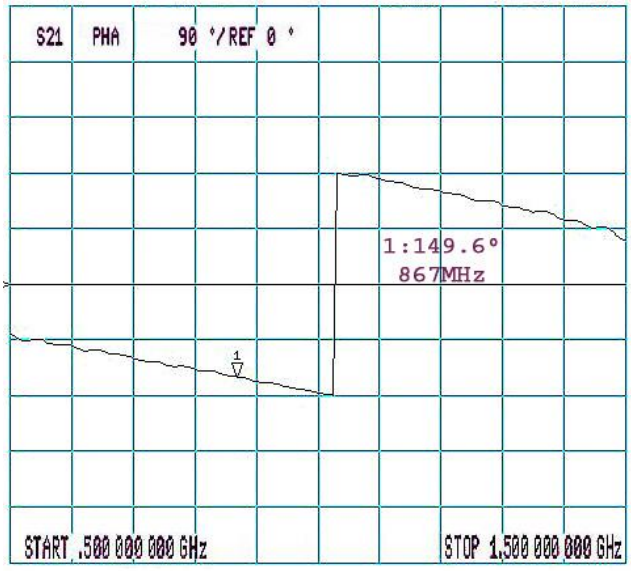

Figure 3.8: S12 (phase)

İn Fig.3.7 and Fig.3.8 phases of reference and delay arm are given. At 867 MHz, S12 phase of reference arm is 88.5°and S12 phase of delay arm is -149.6°, with phase difference of -119.1°.

3.2 Power Divider

Power dividers or combiners are used in various RF applications and antenna arrays are one field of the application of them. Design of feed array networks are one of the most fundamental part of array antenna design which will be investigated in the next chapter. In this antenna array feeding networks power should be divided as desired to the each antenna element while matching each antenna element to the input impedance and, this mechanism of dividing the power and matching the elements is achieved through power dividers.

Due to antenna array structure antenna array requires equal power at all radiating elements, for this purpose equal Wilkinson power divider is implemented. Equal power dividers, divides the power equally between the output ports with minimum possible isolation between them. General structure of Wilkinson power divider can be seen in Figure 3.9

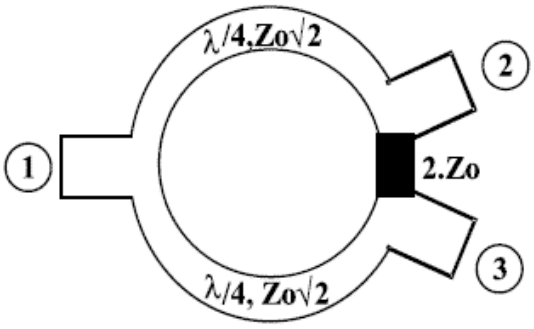

Figure 3.9: Wilkinson Equal Power Divider

Wilkinson power divider consists of four main parts, input port, quarter-wave transformers, isolation resistor and output ports. Input port of each antenna element is desired to match $50\,\Omega$, so, input impedance is also set to Zo=$50\,\Omega$. Quarter-wave transformer is designed with substrate parameters h=1.6mm and ε_r=4.5, for electrical length of λ/4 and resistance of $\sqrt{2}\times 50 = 70.7\ \Omega$. If the isolation level is not adequate or there is low isolation between the output ports, power will not be divided equally. By using the isolation resistance, isolation between the $50\,\Omega$ outputs ports will be achieved, whereas, an isolation resistance $2\times 50 = 100\ \Omega$ is used, which is added between the output ports.

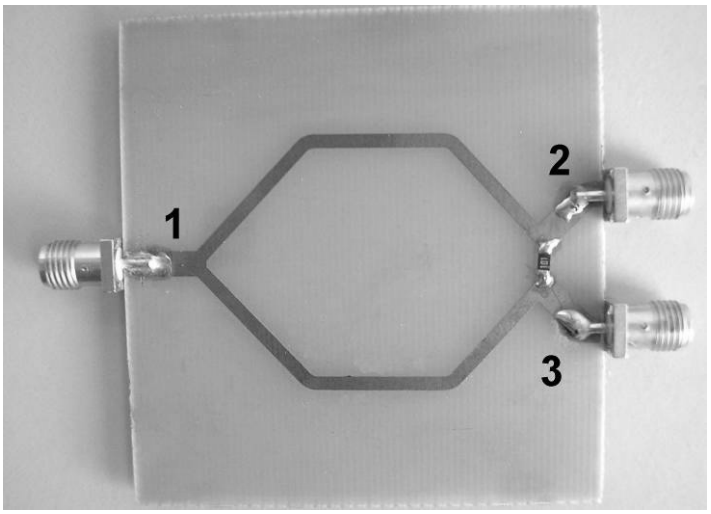

Figure 3.10: Realized Wilkinson Equal Power Divider

Implemented Wilkinson power divider can be seen in Figure 3.10. As an isolation resistance SMD resistance is used. By the use of network analyzer, two ports, measurements are done, and showed in the below Figures 3.11 – 3.15 where port names 1, 2 and 3 are assigned as in the Figure 3.9

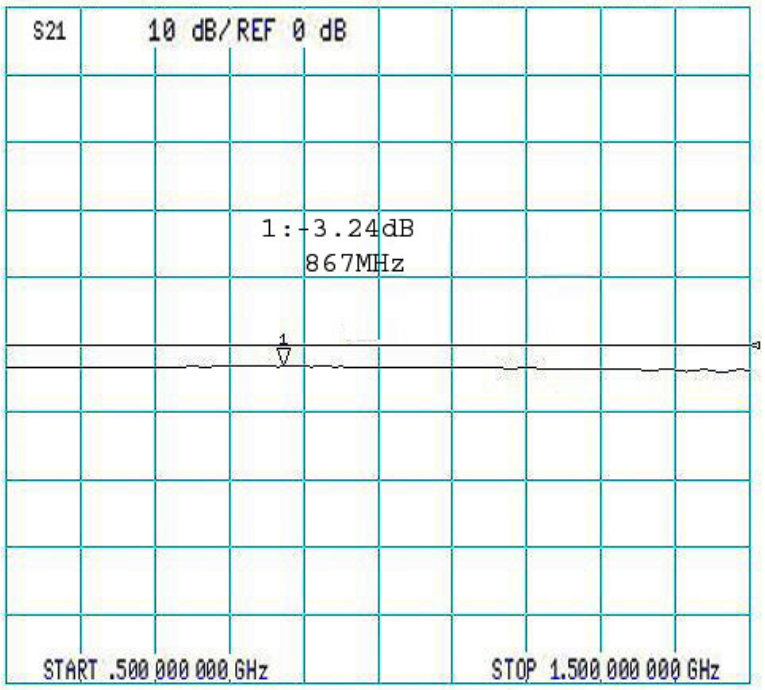

Figure 3.11: S12 (dB)

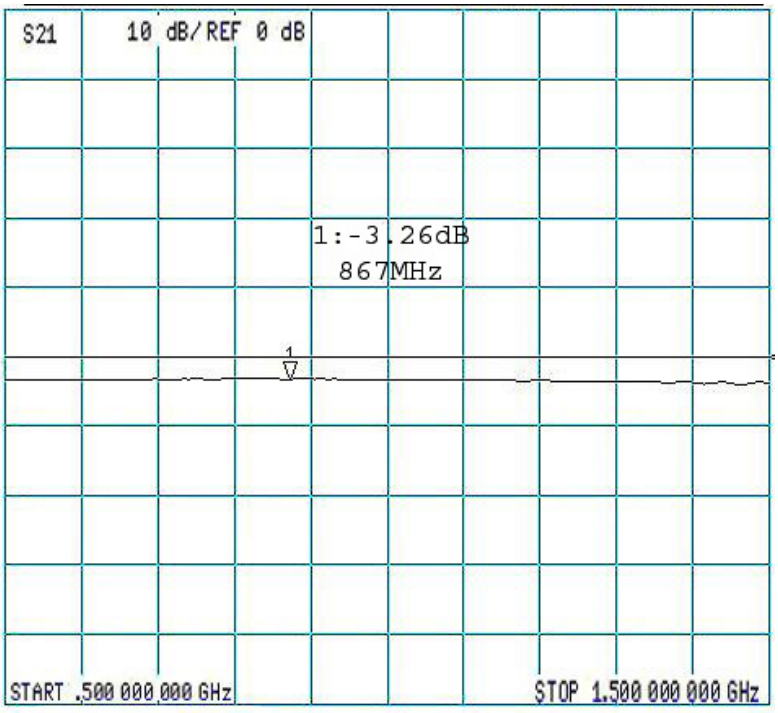

Figure 3.12: S13 (dB)

From the measurement results, it is seen that between the input and output ports power is divided equally at 867MHz. In figure 3.11 and 3.12 at 867 MHz $S_{12} = S_{13} = -3.2dB$ is measured, with an insertion loss of 0.2dB at each port divided power is transmitted equally to the output ports.

Figure 3.13: S22 (dB)

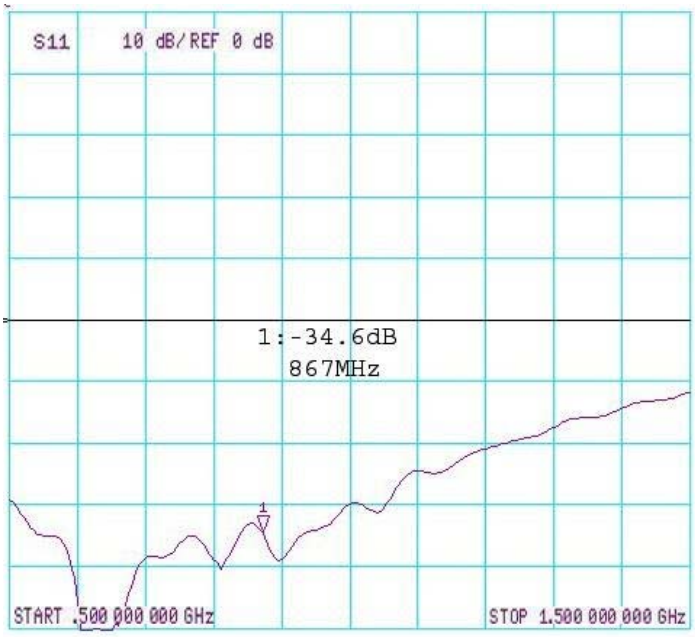

Figure 3.14: S33 (dB)

In the same way, return loss for the output ports are very low at 867MHz. Finally, to see the isolation between the output ports, s-parameter analyses between the port 2 and 3 is done. In the Figure 3.13 and 3.14 S-parameters can be observed as $S_{22} \approx S_{33} \approx -40dB$ for output port 2 and 3. And in the figure 3.14 measurement of return loss of the input port is given and at 870MHz S_{11} ≈ -48dB is measured.

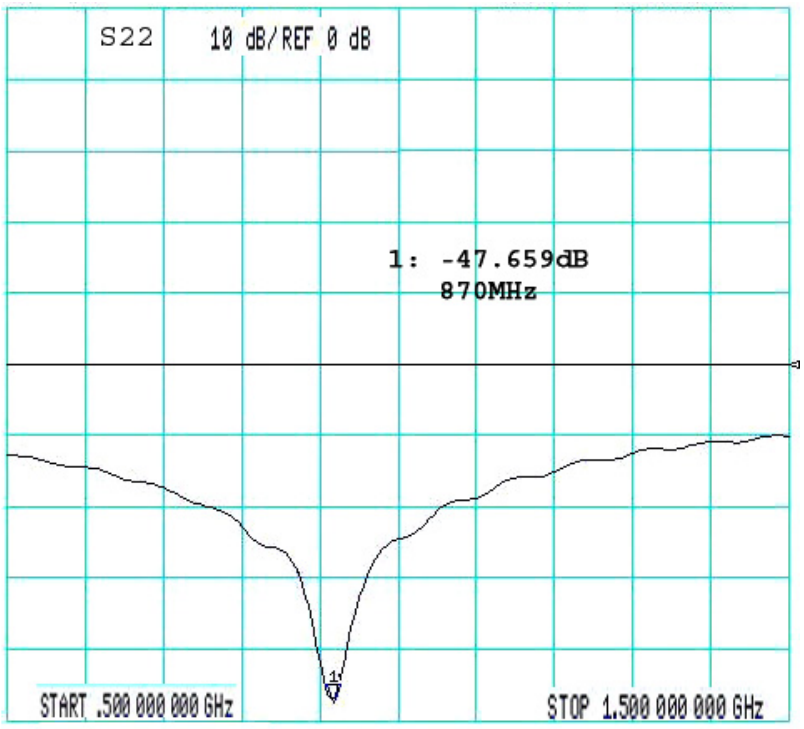

Figure 3.14: S11 (dB)

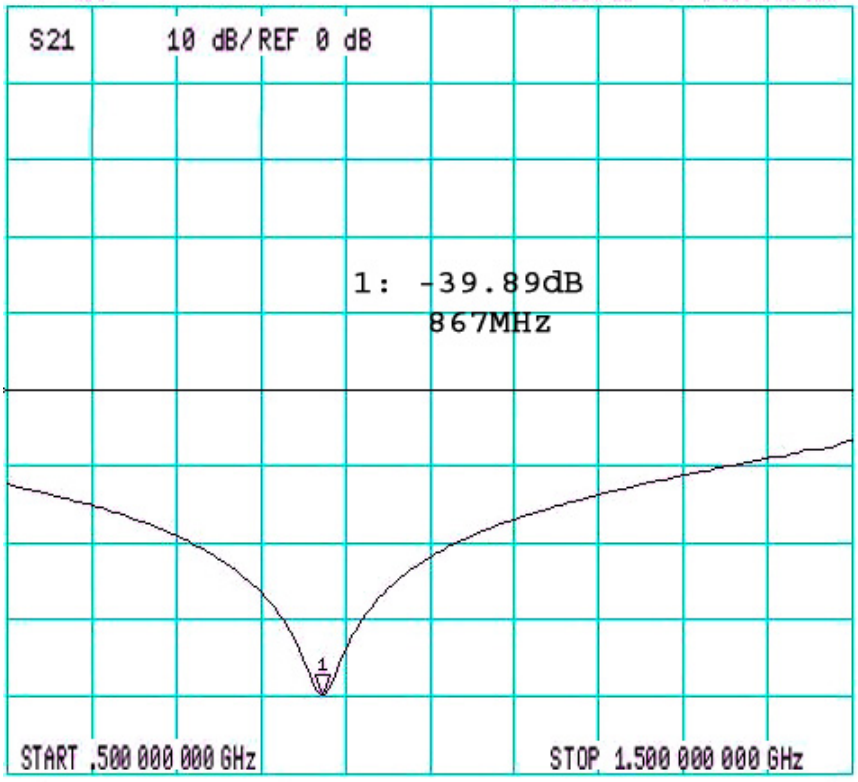

Figure 3.15: S23 (dB)

4. Microstrip Antenna Array

4.1 Why phased antenna array?

The coverage and the operation range of a passive system can be increased by increase in transmit power; however it is not applicable due to regulations. However, by using more directive antenna more far away points can be reached, as it is seen in the Figure 4-5.

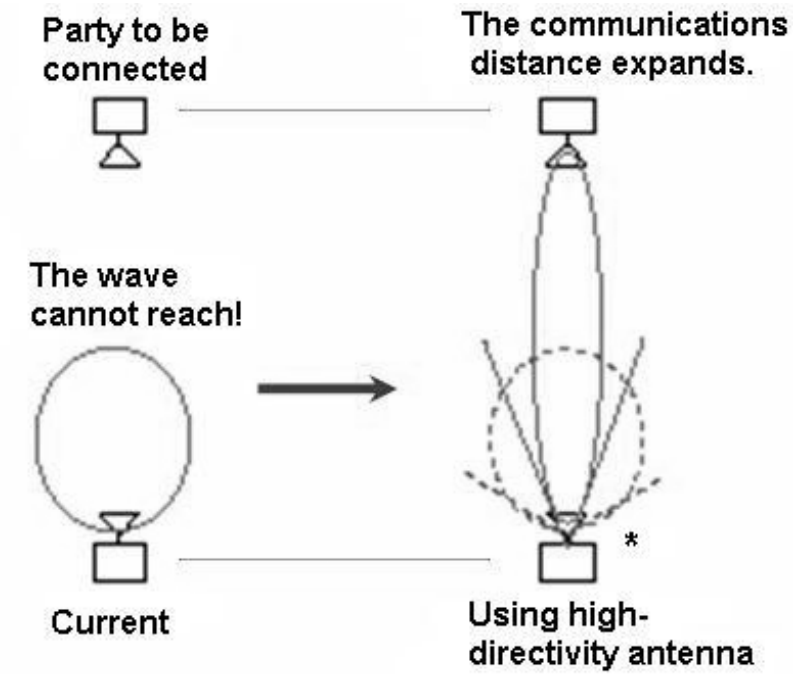

***Using the same transmit power level**

Figure 4-1: Use of directive antennas

By using the same transmit power operation range of the communication channel can be increased. In our approach, one of the antennas of the bi-static

reader will be replaced by the phased antenna array, with a more directive beam with higher gain. Diagram of proposed phased array antenna can be seen in the Figure 4-2, which consists of four (2x2) patch antenna elements, Wilkinson power dividers, phase shifters enabled by SPDT switches.

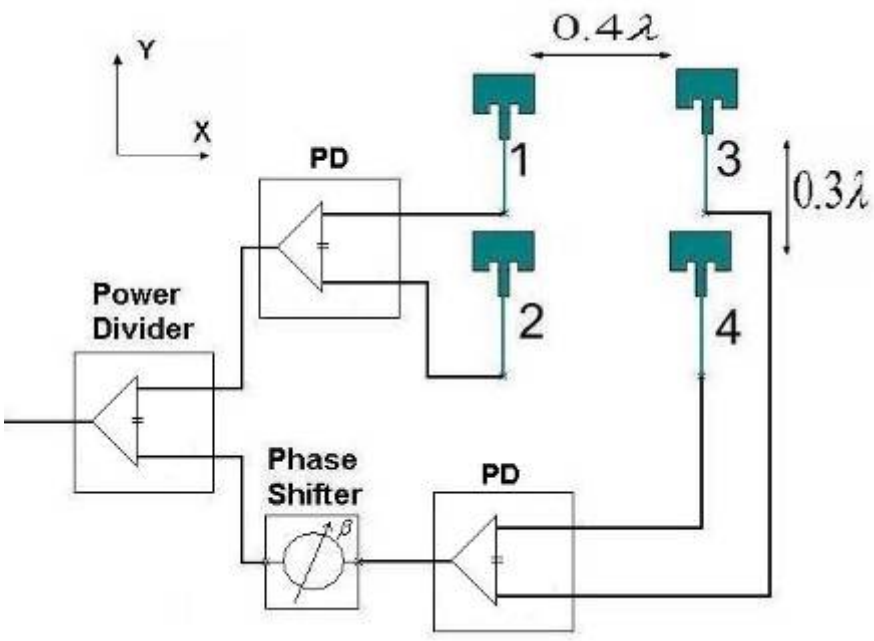

Figure 4-2: Proposed phased array antenna diagram

Increased antenna gain will increase the radial range; however, due to the narrower beamwidth the angular coverage will be decreased. In our technique, by using transmission line phase shifter, the main beam of the phased array can be steered to two main different directions, as shown in the Figure 4-3 as State1 and State2, so that the angular coverage is not affected; instead, it will be extended. A typical radiation pattern of a microstrip patch antenna is shown in Figure 4-3 as radiating into the half space, also shown in the Figure 4-3, a more directive beam of a phased antenna array with two different pointing directions. One might argue that ERP (effective radiated power) will be increased by using high gain antenna; however, if the time average power is calculated, it will be the same as fixed beam less directive antenna because the

beam will be steered back and forth between these two states and decrease the average power. In normal operation, the beam will be shifting between the two states for a predetermined amount of time.

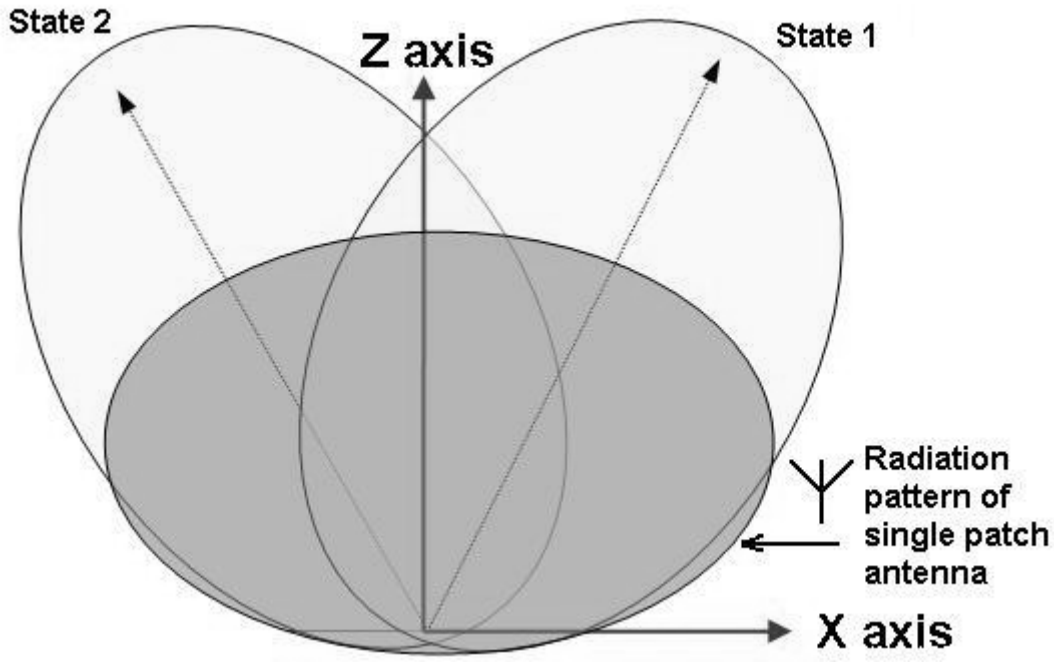

Figure 4-3: Extending coverage and range of operation

4.2 Microstrip Antenna Array

Microstrip antenna arrays comprised of printed patches and printed lines for the feed network represent the goal of much research development activities. The design of microstrip antenna arrays is fundamentally the same as the design of other types of arrays, so ultimately performance is dependent upon achieving the desired amplitude and phase distribution of currents on the elements of the array for all frequencies and scan angles of interest. The effects of mutual coupling can be more significant in microstrip arrays than in some other arrays, leading to scan blindness in severe cases [28], [29]. However, arrays with a

broadside beam are often required in practice, and these arrays frequently can be designed without considering mutual coupling effects [33].

4.3 Array Analysis

Main objective of the design was as denoted before, steering the beam with desired phases to ensure that increasing the coverage and operation range of possible RFID application. The overall antenna pattern of a microstrip patch array is formed with the contribution of each patch element. The antenna pattern of the array could be obtained by multiplying the single antenna pattern with a parameter called Array Factor. Array factor varies with angle differences and it shapes the single antenna pattern to form the overall array pattern. The array factor depends on distances between patch elements, total number of the patch elements, the phase and amplitude differences of the currents between adjacent patch elements and the frequency of the field. For this purpose, to steer the beam as preferred, all this variables should be handled together. In the direction of demands, operation frequency is defined by the application as 867MHz and for 2x2 antenna array (with total four elements), power is determined to be delivered equally. Also, the spacing between adjacent antenna elements of an array should not exceed one wavelength for any frequencies within the frequency bandwidth in order to eliminate the spurious grating lobe occurrence [30]. And to obtain maximum gain, minimum coupling and with minimum area criterion element spacing between the microstrip antennas are selected 0.3 λ_0 in x-direction and 0.4 λ_0 in y-direction. As, it is stated in [31], [32], cross-polarization generated by higher order modes of a patch antenna can be cancelled by proper use of symmetry, elements placed symmetrically with given element spacing in x and y coordination.

4.3.1 Array Factor

To briefly introduce to the array factor calculations done on the Matlab some array factor analysis will be given with regard to our design of 2x2 antenna array. For M elements in x-axis with element spacing d_x with and N elements in y-axis with element spacing of d_y. Also for phase shift of β_x between the elements in x-axis and phase shift of β_y between the elements in y-axis is defined. Moreover, element excitation are given as I_m in the x-axis and I_n in the y axis. Than array factor of the planar antenna array can be written as in Eqn.4.1 [21].

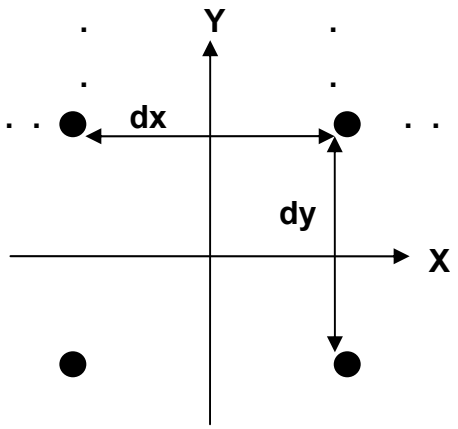

$$AF = \sum_{m=1}^{M} I_{m1} e^{j(m-1)(kd_x \sin\theta\cos\phi+\beta_x)} * \sum_{n=1}^{N} I_{1n} e^{j(n-1)(kd_y \sin\theta\sin\phi+\beta_y)} \quad (4.1)$$

After choosing two parameters of the phased array antenna, as a last parameter, to calculate the array factor phase difference between the antenna branches for beam steering is needed to be calculated. Array factor calculations are done in Matlab and it is determined that to obtain the beam steered at ±30° degrees, phase difference of ±120° degree is needed between the branches in x-direction.

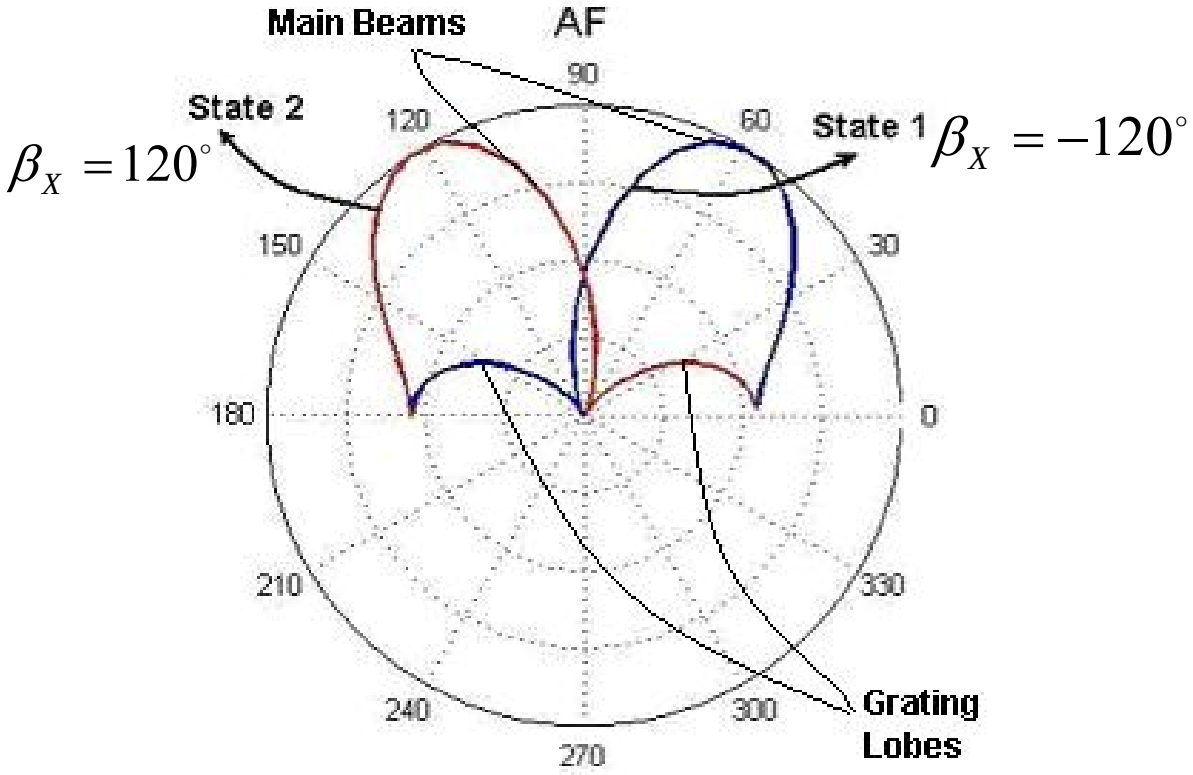

Figure 4-4: Array factor calculations

In the Figure 4-4 array factor pattern for both ±120° degrees is plotted for states 1 and 2 as related with phase differences in the above plot. As it is mentioned, array factor is shifted between ±30° degrees for state 1 and 2 as desired.

However, this will not give final radiation pattern of the antenna array, but implies about it, because, overall antenna array radiation pattern is characterized by multiplying of radiation pattern of single microstrip patch antenna and the array factor. So, we can suggest that, overall radiation pattern will be also shifted between ±30° degrees but beamwidth will be broaden with the effects of microstrip patch antenna, also, side lobes can become larger on the overall antenna array radiation pattern. If we again come back to the examination of antenna array in schematic environment, to analyze the feed network, microstrip antennas are replaced by 50Ω output ports. Also, without adding the phase shifter to the feed network layout, the essential phase simulations could be done, due to transmission line phase shifter will be added to the feed network without adding any enlargement in terms of length of lines.

4.3 Schematic Analysis

Design, simulations and measurements of microstrip patch antenna, transmission line phase shifter and Wilkinson equal power divider is given individually. In this chapter antenna array structure and array feed network will be investigated. At first circuit schematic of antenna array is designed and simulated.

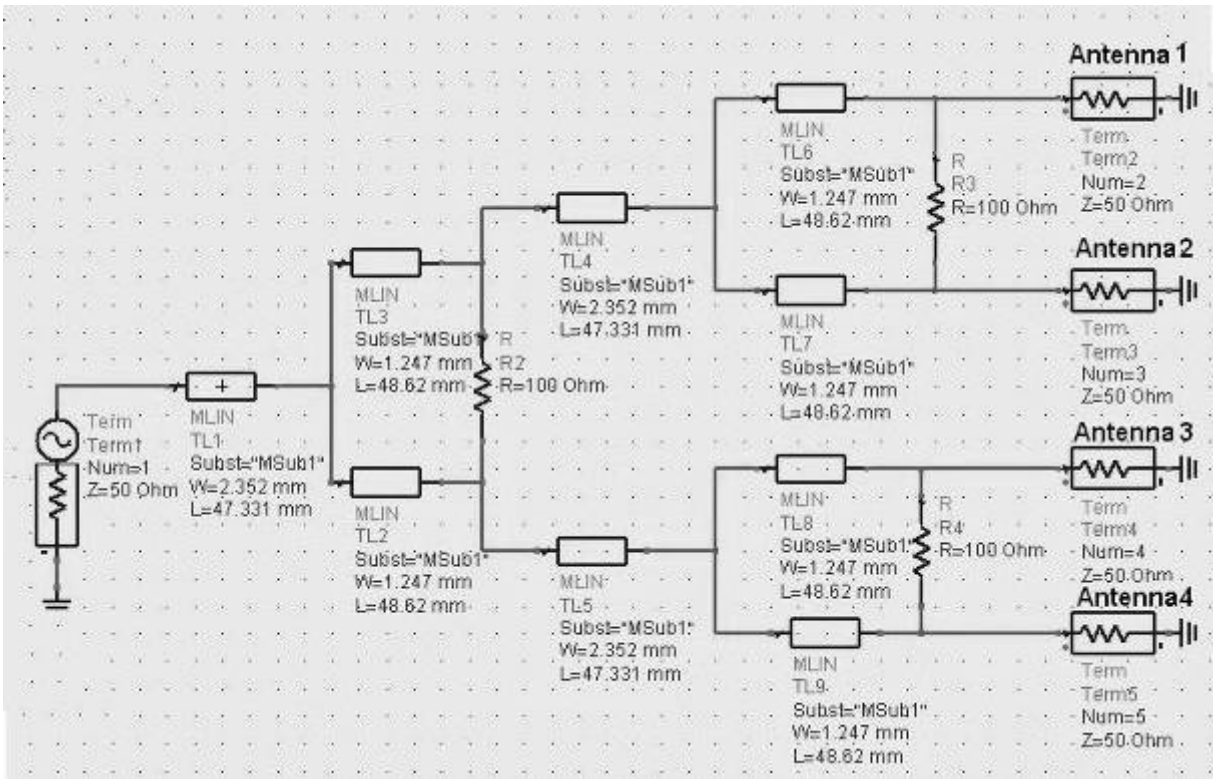

Figure 4-5: Schematic view of Antenna Array

Powers delivered to the antennas are all equal, except the phase shifter which is needed for beam forming, all the elements of the antenna array circuit is simulated in the schematic (Figure 4-5). In terms of antennas, 50Ω ports are defined, for this schematic simulation s-parameter analyses completed as shown in Figure 4-6 to Figure 4-8.

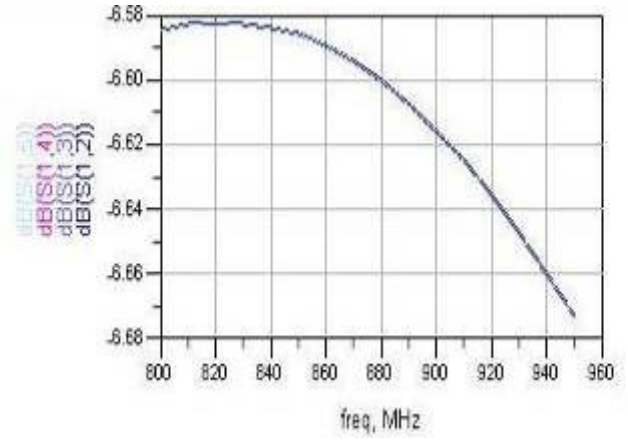

Figure 4-6: S12, S13, S14, S15 dB

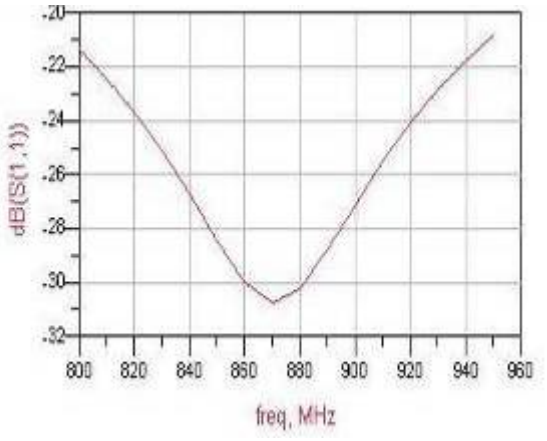

Figure 4-7: S11 dB

In Figure 4-6, power delivered to output ports, which corresponds to each microstrip antenna elements, from the input port, is plotted. For the correct values of electrical length of λ/4 at 867MHz of Wilkinson power divider, power is divided to four in two steps with an insertion loss of 0.6dB. In Figure 4-6, return loss of input port is plotted, at 867MHz return loss measured -30dB which means 99.9% of power is transmitted.

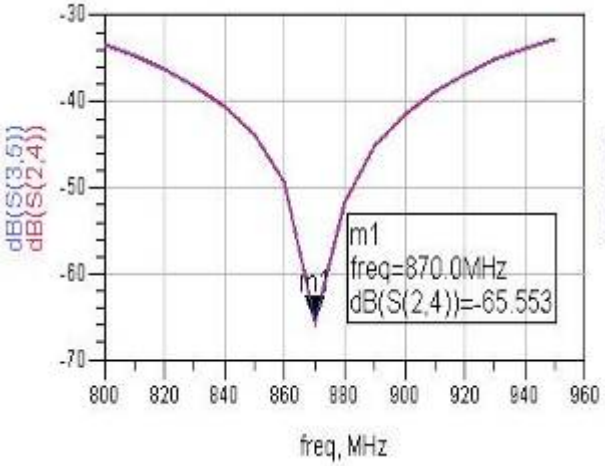

Figure 4-8: S24, S35 dB

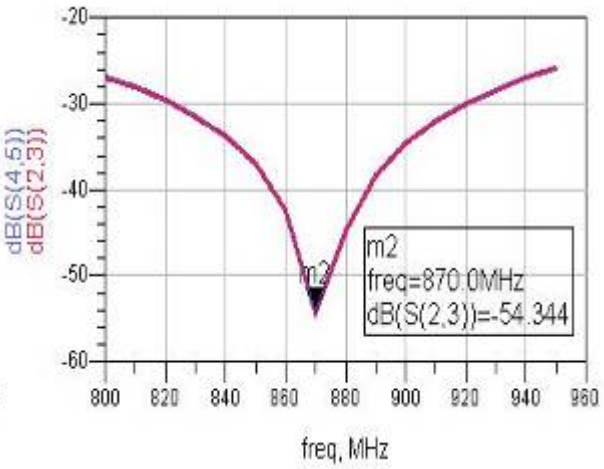

Figure 4-9: S23, S45 dB

After the input power is divided and delivered equally to the output ports is ascertained, isolation between the output ports are investigated between the

inner and the outer branches. In the Figure 4-8 isolation between the outer branch ports are plotted, ex: Antenna 1 vs. Antenna 4 and Antenna 2 vs. Antenna 3. In the Figure 4-8, isolation between the inner branch ports are plotted, ex: Antenna 1 vs. Antenna2 and Antenna 3 vs. Antenna 4. With these two stages of feed array network, and with use of three Wilkinson power dividers, power divided equally with very low insertion loss and high isolation between the outputs ports, this point also verified in the actual power divider measurements in the chapter 3. In the schematic, previously measured 50Ω and 70Ω transmission lines in the power divider section, are used. Measurements and more detailed results of power divider are given in that section. Transmission line phase shifter is not added to the antenna array feed network schematic model. Structure of the transmission line phase shifter will not add any differentiation in terms of schematic analysis. After completing the schematic simulations of the antenna array feed network layout in ADS Momentum is drawn and analyzed.

4.4 Layout Analysis

After schematic simulations, it is seen that power is delivered equally to the microstrip antenna ports, layout simulations of whole antenna array is analyzed to ensure that necessary phase shift is obtained between the antenna branches to able to steer the beam ±30° degrees and with a minimum insertion loss on the feed network.

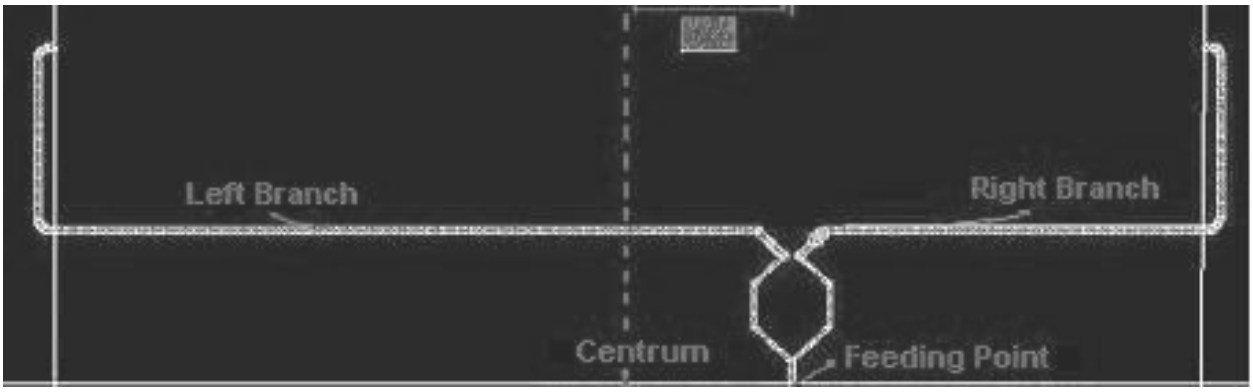

Figure 4-10: Antenna array feed network layout

Because the phase shifter will obtain ±120° degree phase difference, between the antenna branches in x-direction ±240° phase difference is needed. Thus, feed point of the antenna array is shifted λ/3 in x-direction which will supply the 2λ/3 phase difference. As shown in the plot at right side, with this feed network scheme and with the use of phase shifter, phase will be steered for desired beam states.

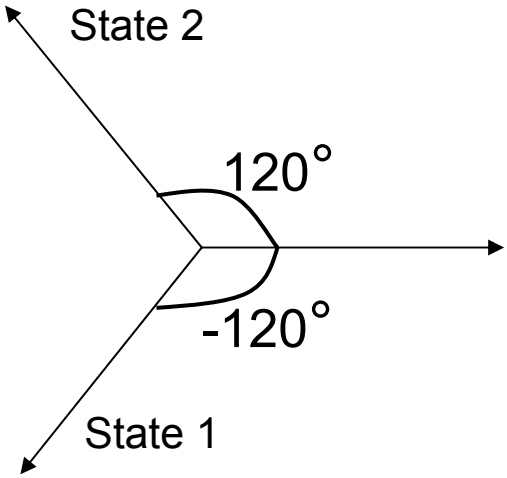

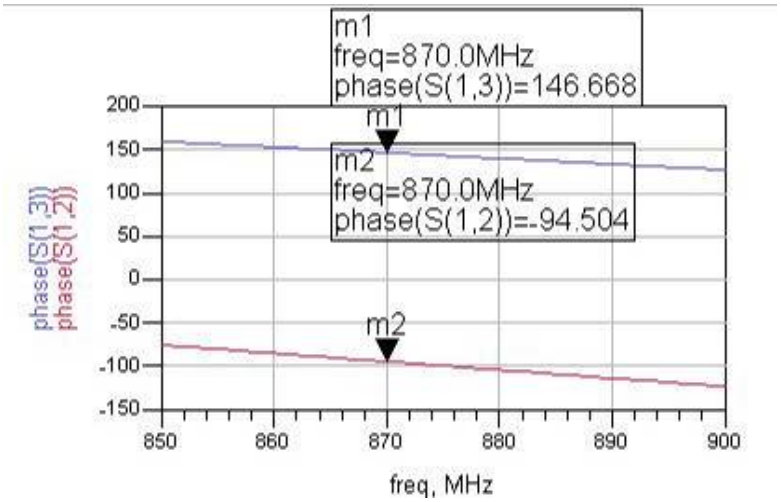

Figure 4-11: S12 – S13 phase

Firstly, in the Figure 4-10 phase of the network is analyzed and the simulations of the phase difference between the input port and output ports 2 and 3 are given in Figure 4-11. For this feed network scheme return loss of input port of -32dB is measured at 867MHz in Figure 4-12 which are very close to the schematic simulations.

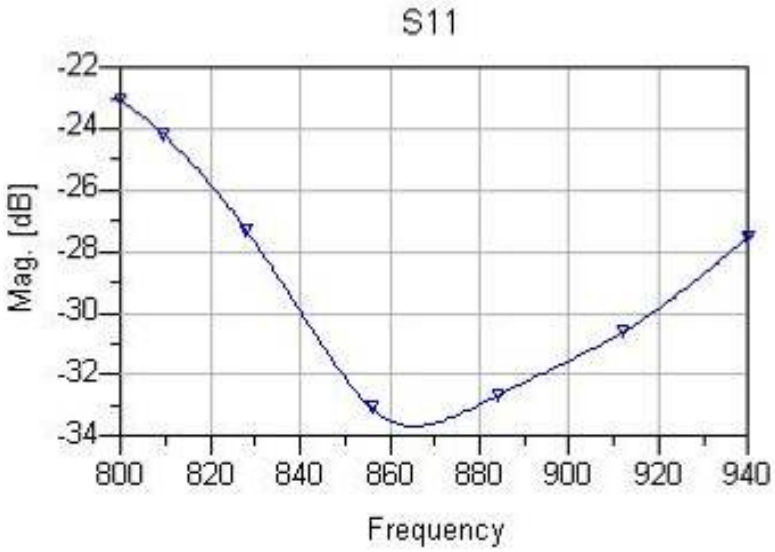

Figure 4-12: Return loss of input port

After completing the ADS schematic simulations of the antenna array feed, and understanding both that input port has low return loss and input power is delivered equally to the antenna output ports. In the layout simulations of antenna array feed network, after it is confirmed that, right and left branches have necessary phase difference to obtain necessary array factor, complete antenna array layout analysis is performed. In the antenna array layout analysis, switch is not included to the layout, because in the ADS layout environment active devices like switches can not be included in the analysis, only if it is desired, it can be just added to the S-parameter analysis, but not to the full wave EM simulations. The antenna array with phase shifter can be seen

from Figure 4-13, however in the analysis switch is not used. Instead physical connections are made for the simulations of the switch.

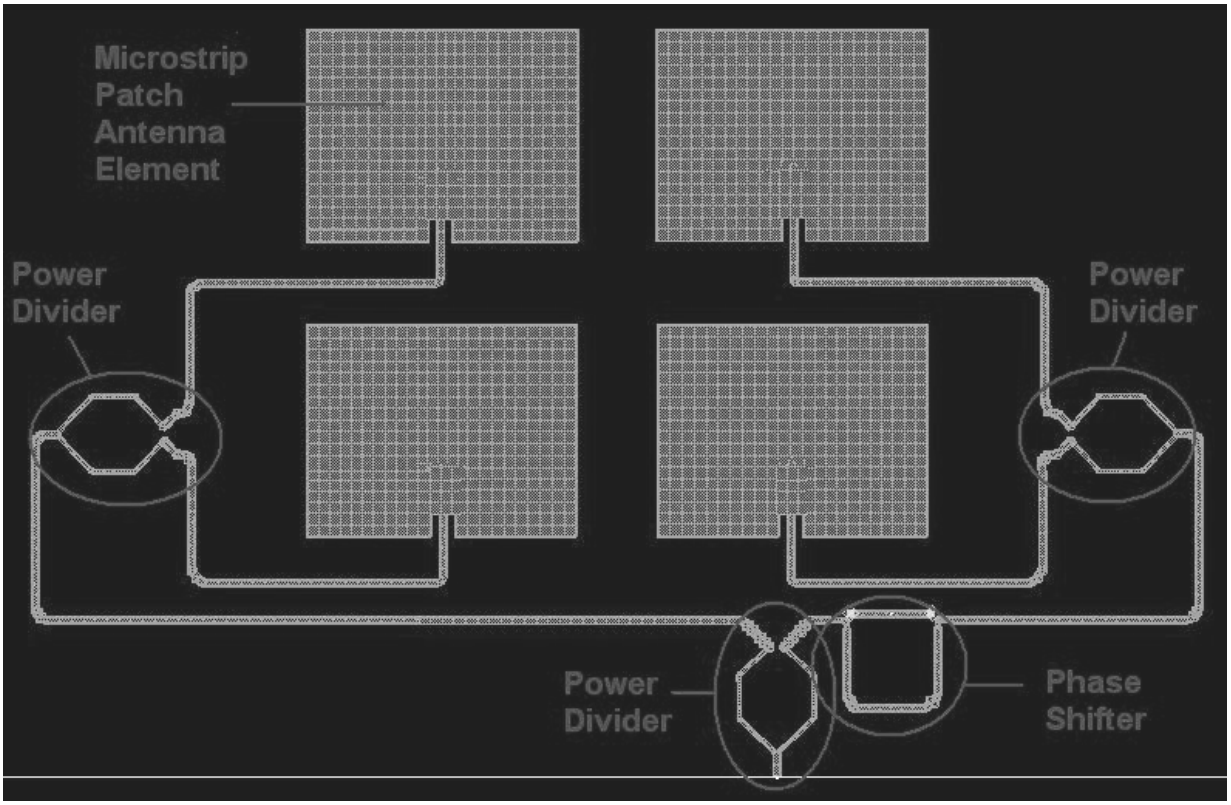

Figure 4-13: Layout of antenna array

4.5 S-Parameter Analysis

After completing the whole layout design of antenna array with necessary phase differences between branches and element spacing, S-parameters are obtained. In the Figure 4-14 and Figure 4-15 return loss of input port for two states of the antenna is given.

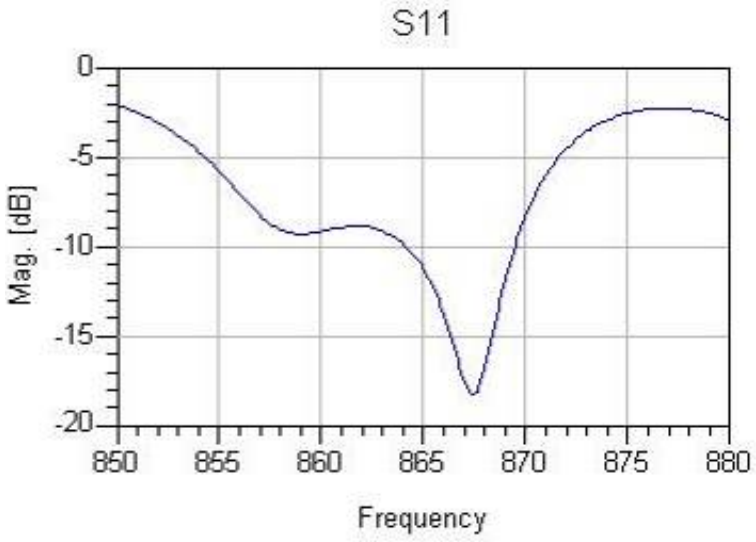

Figure 4-14: S11 (State 1)

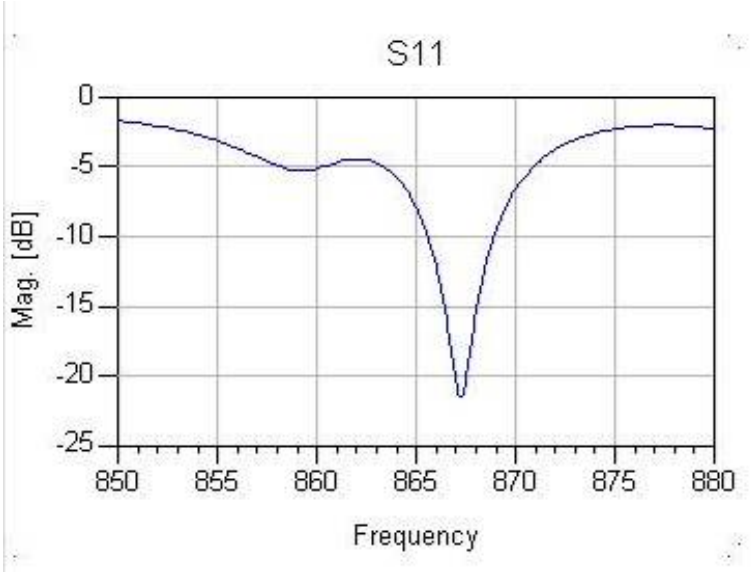

Figure 4-15: S11 (State 2)

Return loss of around -25dB, -27dB for state1 and -22dB for state2, are obtained for both at the 867MHz. Also, around 867MHz, more than necessary bandwidth for the RFID application which is 2MHz is achieved. Additional out of band loss can be observed compared to the return loss of single microstrip patch antenna, due to the additional long feeding network transmission lines.

4.6 Radiation Pattern Simulations

After the S-parameter analysis, to investigate the main beam radiation direction far fields of the array calculated for two different position of the switch that antenna array radiates for two states of the antenna in 867MHz, radiation pattern is calculated. Radiation plot results for H-plane for the two states of the antenna are given in Figure 4-16 and Figure 4-19.

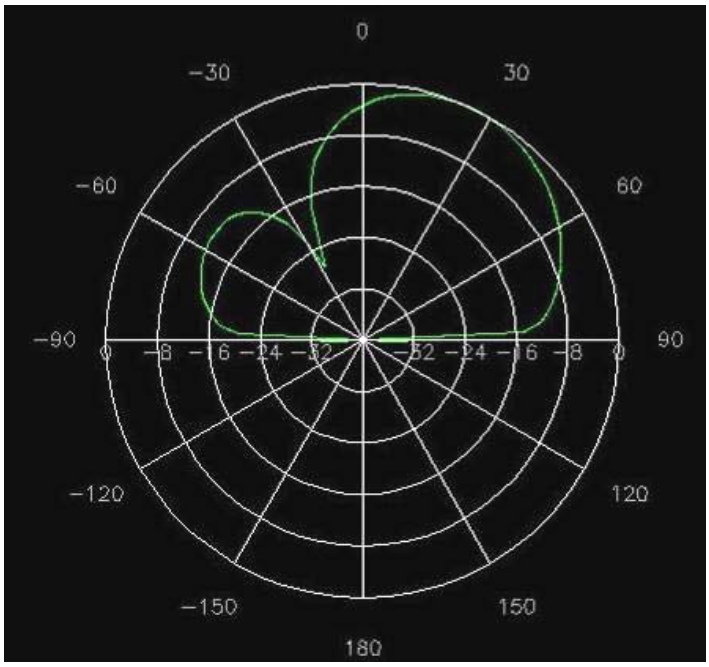

Figure 4-16: H-plane polar radiation plot (State 1)

When the switches pass the signal from reference arm of the phase shifter which corresponds to the state 1, H-plane radiation pattern is obtained in Figure 4-16. Main beam is obtained at 30° degree and side lobe is appeared at -50° degree. And 2D plot of the H-plane radiation pattern with cross polarization is plotted in Figure 4-17. Between the main beam and the side lobe more than 10dB difference is obtained with a co-cross pol difference of better than 30dB in the main lobe. Furthermore, 3D view of the far field radiation pattern for the state 1 of the antenna array is given in Figure 4-18.

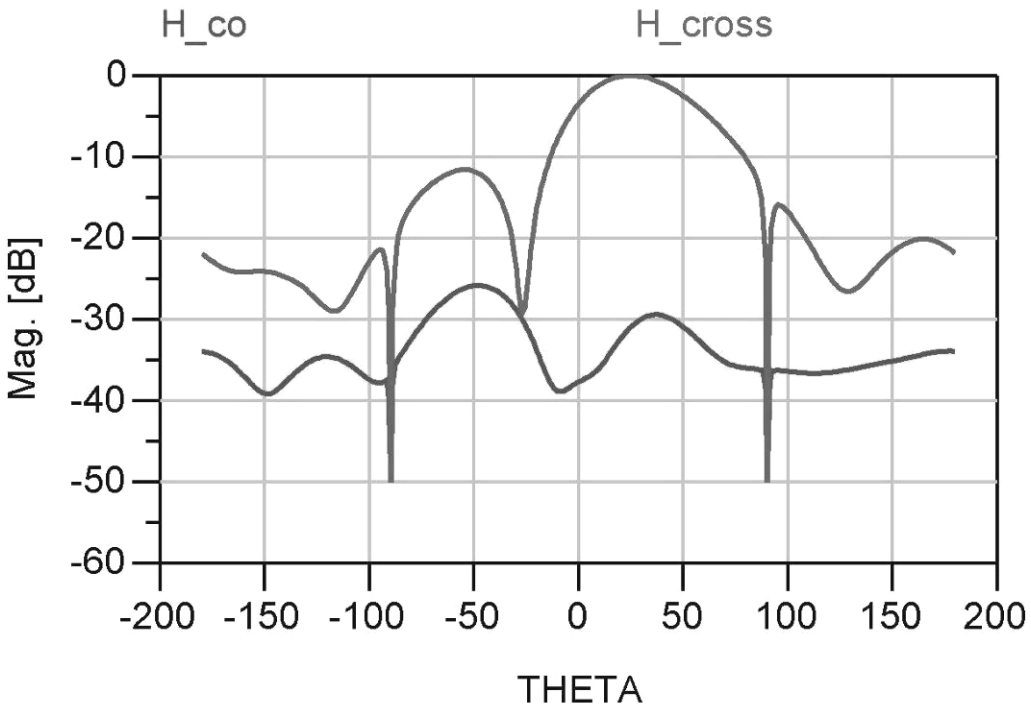

Figure 4-17: Co-Cross Pol H-plane radiation pattern (State 1)

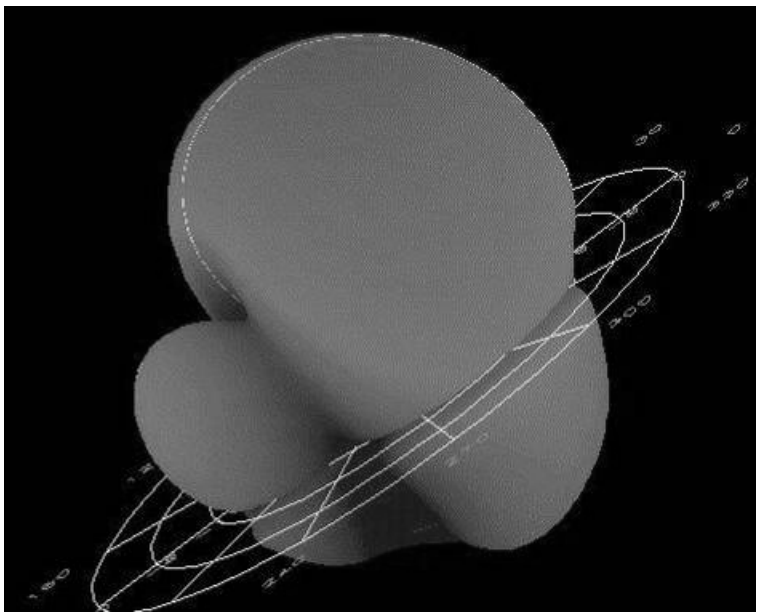

Figure 4-18: 3D far field radiation plot (state 1)

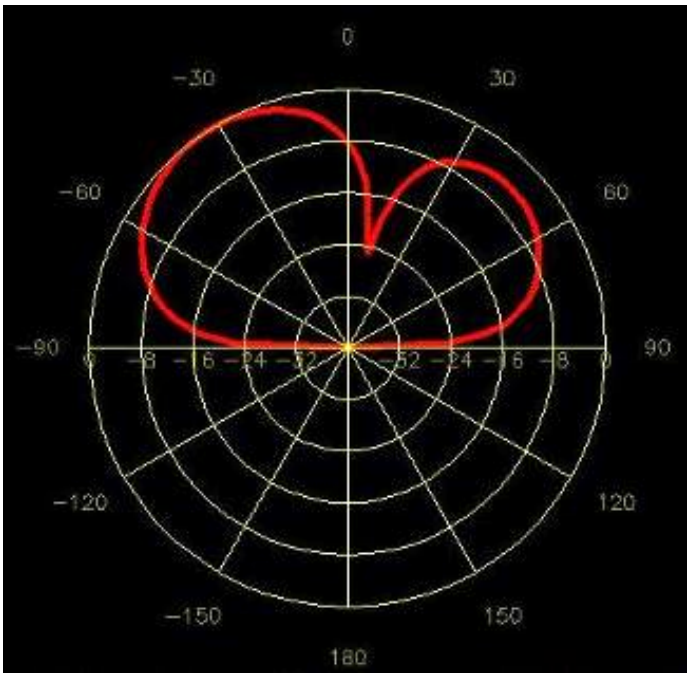

Figure 4-19: H-plane polar radiation plot (State 2)

For the state 2, switches at the phase shifter are open for the reference arm, H-plane is plotted in Figure 4-19, it is observed that main beam is steered to -30° degree and side lobe is obtained at -50° degree.

Because it is desired to steer the beam in H-plane and array factor is steered just in elevation pattern, there is no difference between both states of the antenna array in the E-plane as plotted in Figure 4-20. 2D and 3D plots for state 2 is not plotted. Figure 4-20 represents e-plane radiation for both of the states.

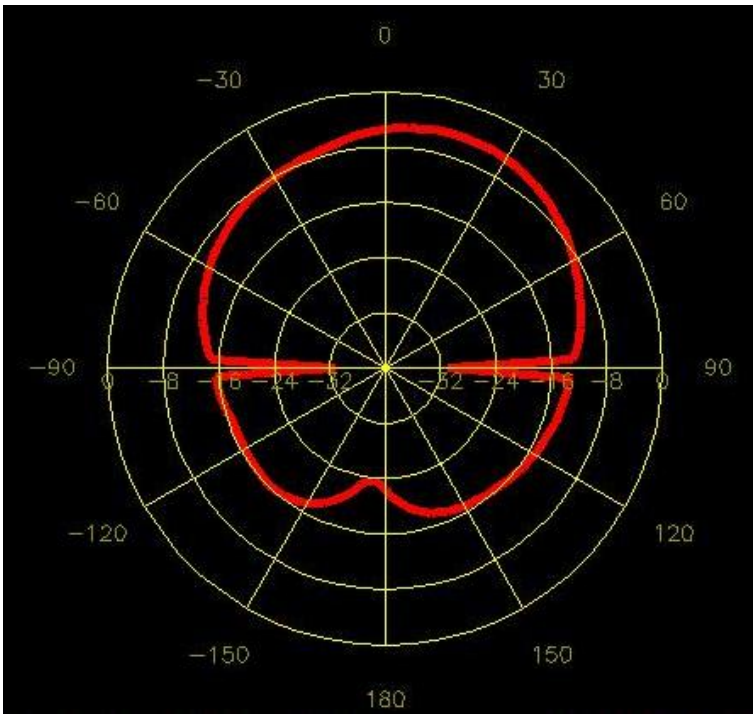

Figure 4-20: E-plane polar radiation plot

4.7 Measurements

After seeing that array antenna radiates at 867MHz in two states, and beam is shifted between ±30 degrees, antenna array is printed on low loss PTFE woven-glass ceramic composite Nelco NH9450 substrate with dielectric constant of 4.5, height of 1.52mm and tangent loss of 0.002. Both side of the substrate is coated with 35μ thickness electro-deposited(ED) copper.

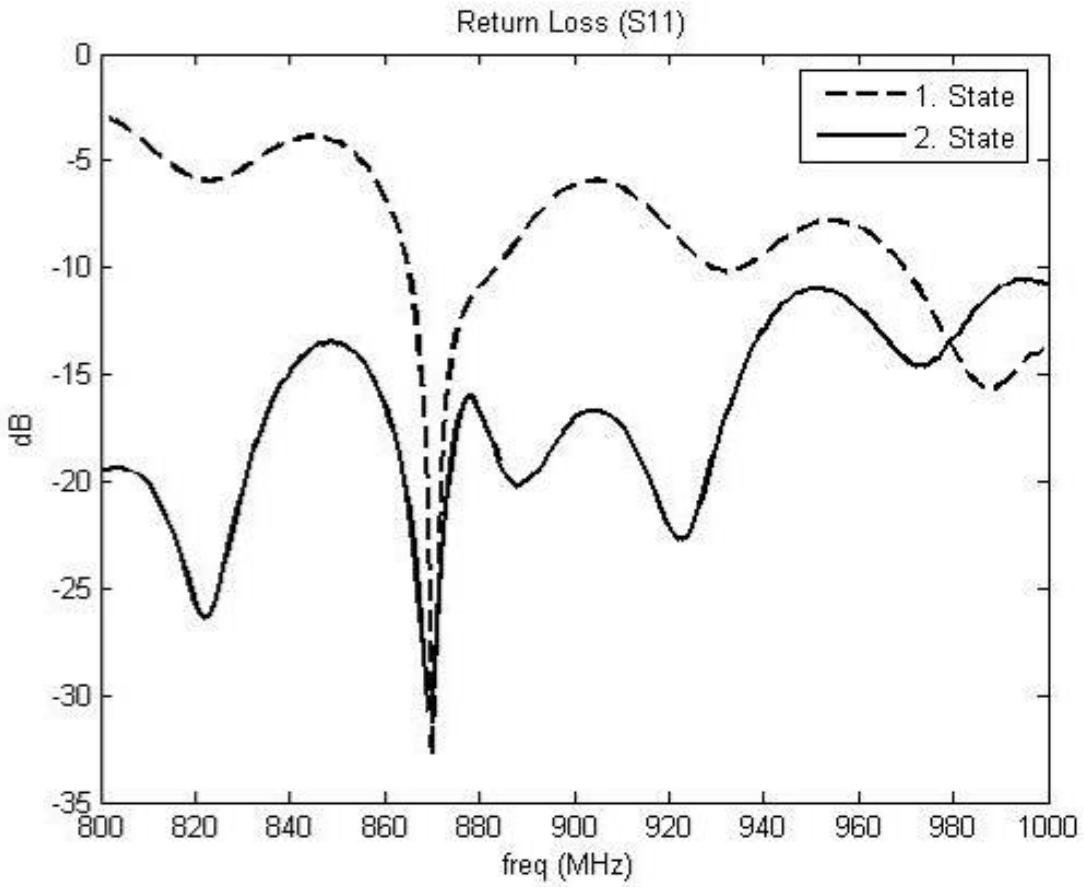

Figure 4-21: Return loss of antenna for (State 1 and 2)

S-parameters of the antenna array are measured in network analyzer, and return loss of input port for the two states of antenna array is plotted in the Figure 4-21. It is seen that for two states of the antenna array radiates in 867MHz, and except the out of band losses simulation and measurement s-parameter results are matched. Difference in terms of losses can be accounted to the conductor and dielectric losses which are not examined adequately enough with the ADS Momentum that can cause to the surface waves above the substrate. Dielectric losses is mainly based on the tangent loss of the substrates which is evaluated by ADS Momentum, however conductor losses is based on skin effect and surface roughness, which could be increased during manufacturing process. After the S-parameter measurements, and understood that antenna array radiates at 867MHz in the two states, to characterize

radiation properties, radiation pattern analysis of antenna array is done in the compact test range facilities of TUBITAK UEKAE. First two plots are plotted for H-plane of the antenna, which is the main concern from the starting point to increase the coverage and the operation range. Without even looking in detail it can be seen that in radiation on azimuth angle is steered as expected from the simulations. Last plot is given for the elevation pattern of the radiation which is both same for the two states.

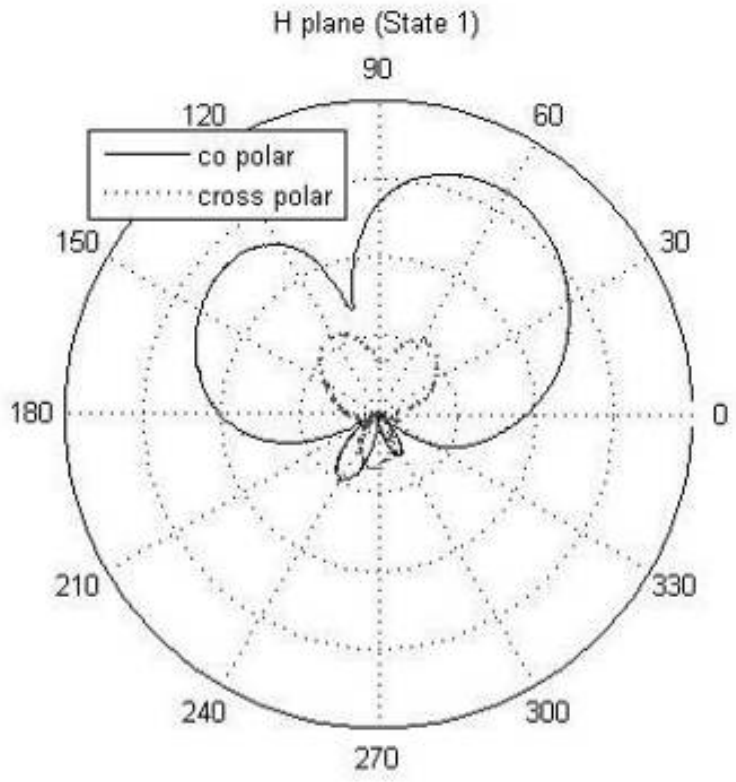

Figure 4-22: Measured co- and cross-polarization (H-plane) for State 1

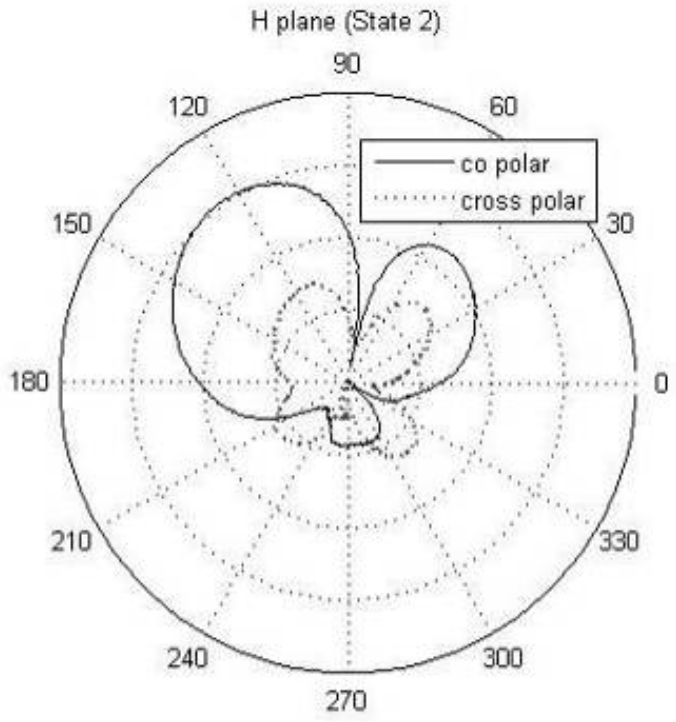

Figure 4-23: Measured co- and cross-polarization (H-plane) for State 2

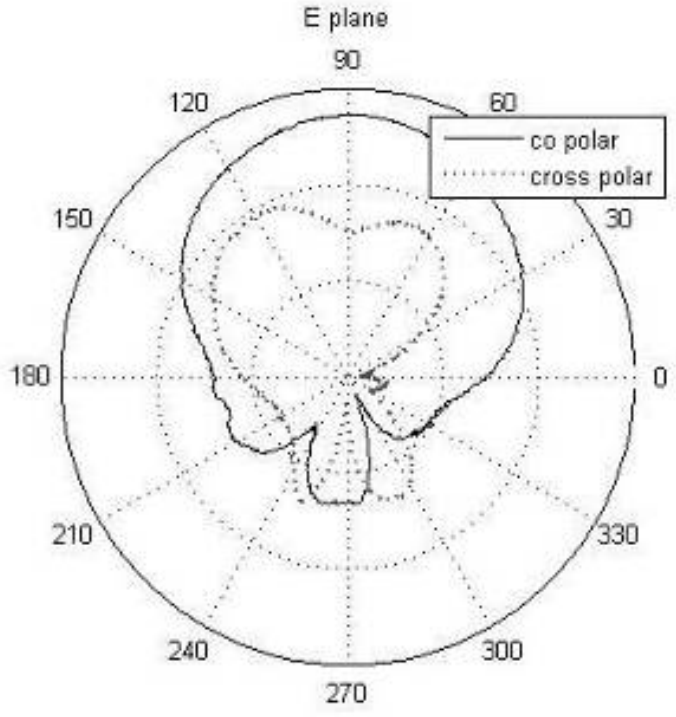

Figure 4-24: Measured co- and cross-polarization (E-plane) for both states

The measured radiation patterns of H-plane of the array for two different states of switches are shown in Figure 4-22 and Figure 4-23, and measured radiation patterns of E-plane is plotted for both of the states together in Figure 4-24, because they have the same characteristics in E-plane. 3dB beamwidth of H-plane for state 1 is 46°, and for state 2, beamwidth is 48°. For E-plane, when upper switches of phase shifter are open, half power beamwidth is 69.3° (State 2), and otherwise, beamwidth is 73.6° (State 1). In accordance with simulation results, directivity of 12.1dB and 20dB difference of co and cross polar level at boresight is obtained at 867 MHz from the measurements. The measured results show that antenna beam can be steered ±30° degrees.

4.8 Experimental results

A test bench to assess the performance of a phased array antenna in an actual RFID system and to confirm the radiation pattern measurements, which shows that antenna beam can be steered ±30° degrees completed in the compact range, has been established. For testing purposes, Alien bi-static ALR-8800 model reader and passive UHF ALN-9554 tags have been used [34]. The array antenna was employed in the receiver port of RFID reader and a standard patch is employed for the transmission port as shown as in the Figure 4-25. Also, to get more accurate results floor of the room is marked densely to easily spot the locations. For different positions of receiver antennas, the standard patch antenna and antenna array in two different states, measurement results affirm the extended coverage and gain of antenna array as compared to those of the patch antenna, as it is plotted in Figure 4-26. Due to the limited area for measurements transmitted power level decreased by 6dB to 0.5watts from the max power level obtainable from RFID reader (2watts), in order to minimize the coverage, and so, increasing reliability of the measurement. Also, for affirmation purposes this read rate test is done for the two different localization of receive antenna. For different positions of the tag in the room it is checked

whether it is read or not read by the reader, and according to the receiver antenna it is noted with different symbols. To represent the two states of the phased array antenna and the standard patch three different symbols are used, which are circle, triangle, and cross. In the Figure 4-26, circles and triangles represent location information when antenna array is used. For the first figure circles represent the state 1 and triangles represent the state 2 of the antenna array, vice versa for the second graph. And, crosses represent the location information that is read by the standard patch antenna. In the first plot reader and transmitter antennas replaced in the opposite sides of the room and in the second plot two antennas placed in the near two side of the room. And, in the both of the plots receiver and transmitter antennas showed as RX and TX.

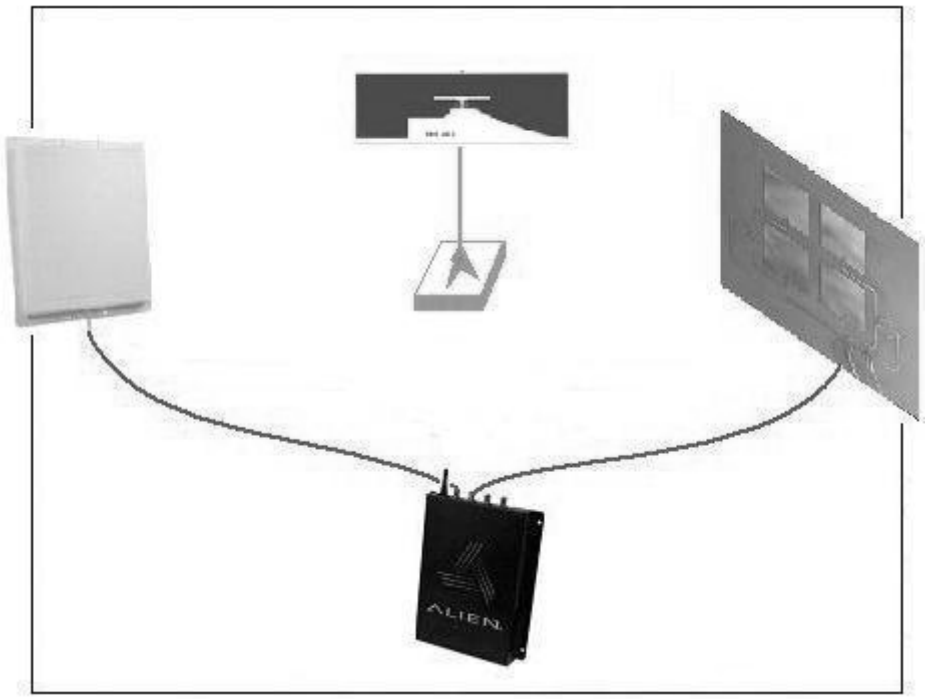

Figure 4-25: Test bed with RFID reader

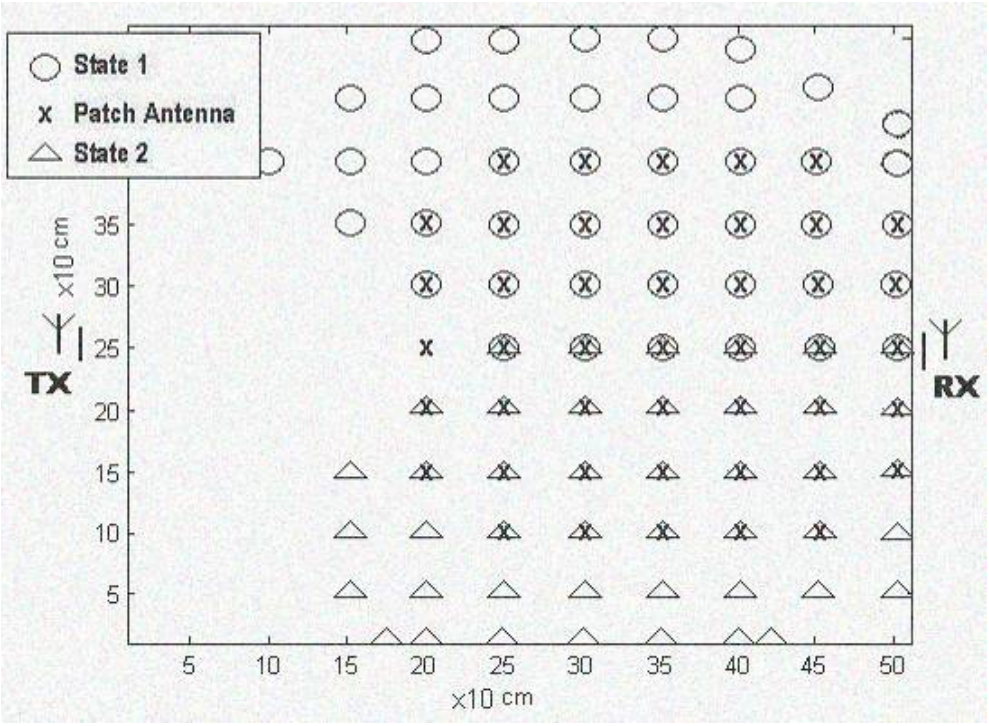

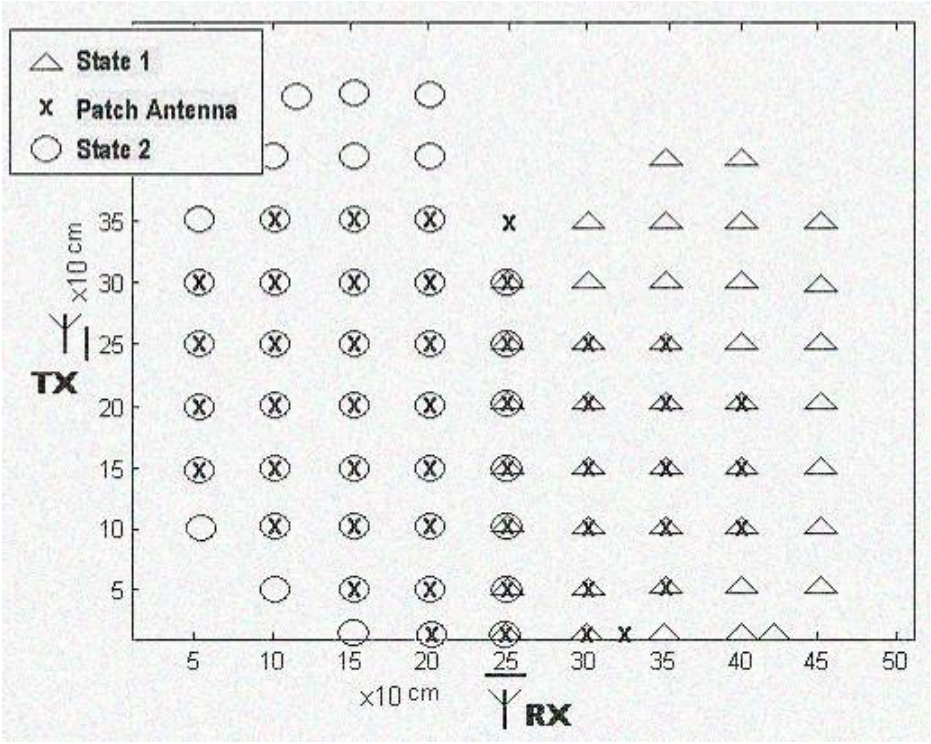

Figure 4-26: Readable location information of UHF passive tags

5. Conclusion

Everyday a new application of Passive RFID system are emerging due to its various advantages like low cost, easy manufacturability and very small size of the tags, besides, able to implement together with the sensor devices which will power up the simple identification devices, with some additional sensor features. So, this field of the technology is very open to the new ideas, and limited by our imagination. However, among other adversary technologies low operation range and the coverage is one of the most important disadvantages of UHF RFID systems.

In this thesis, phased antenna array for passive UHF RFID is designed, implemented, measured and tested. To design phased antenna array, feed network is designed first, which will maintain necessary amplitude to each radiating element and phase difference between them. Feed network design includes also, the separate investigation of phase shifter and power divider, which are designed, implemented and measured one by one. Also as a last substructure radiating element microstrip patch antenna element is designed and implemented. After calculating for maximum gain and minimum coupling and space with use of full-wave electromagnetic simulator ADS Momentum final array structure with use of phase shifter, power divider and microstrip patch antenna, to obtain beam steering between ±30 degrees, the antenna array is implemented on PTFE woven-glass ceramic composite substrate with dielectric constant of 4.5. All the measurements of the antenna array is done, it seen that simulations and the measurements agree with each other. S-parameter measurements are done using S-parameter network analyzer in our

labs. From the radiation pattern measurements which are accomplished in the compact test range facilities of the TUBITAK and experimental test results which is obtained in through use of antenna array in an actual RFID system read rate measurement of the passive RFID tags are completed , it is observed that operation range and coverage is increased. It is seen that compact test range and field tests of antenna array, are consistent with each other. As a another important point, one can ask due to time averaging while steering between the main beams, without causing any issue with the ETSI regulation limits on ERP (effective radiated power) operation range and coverage can be expanded.

As a future work, the increase the number of the antenna element can be one possible way of improvement. However, this will increase the gain and so the operation range, however, size of the antenna array becomes immensely large in the UHF band. Also, with much more element, scanning the area to increase the coverage could be more problematic due to much more steering angle points will need be added to cover the area and it might not be feasible to implement phase shifting for all of this angles and scan them in a certain amount of time, which could decrease the read rates of the RFID tags. Except RFID application perspective, this thesis could be base for other antenna array projects maybe in the higher frequencies where much more antenna elements can be added, and large arrays can be implemented. Because there was no bandwidth requirement for RFID application, bandwidth was not concerned so much in this antenna array design; even the bandwidth of the high Q single layer microstrip patch antenna was enough for the bandwidth requirements. However, for high bandwidth applications, to design an antenna array, other design techniques should be used to increase the bandwidth of the single antenna element and so the whole antenna array. Because there could be different applications which need more bandwidth or gain, more complex structures than simple microstrip antenna, which could be implemented as a radiating element to be in an antenna array. That is to say, for more gain and

bandwidth requiring applications as an antenna element more superior in terms of gain and bandwidth performance can be developed. To epitomize, multi layer EBG (electromagnetic band gab) structures using meta-materials [36], or by using materials with very high permittivity [38], or stacked structures with use of parasitic elements [37], or using AMC (artificial electromagnetic conductor) surfaces [39], or even combining microstrip antenna and PVC horn [40], are examples that will develop in terms of gain, bandwidth or both with a cost of design and implementation complexity and cost increment. However by this way the number of array antenna for the same gain can reduced and array antenna can be miniaturized.

6. References

[1] K. Finkenzeller, *RFID Handbook*, 2nd edition, John Wiley & Sons, England, 2003.

[2] Weinstein, Ron. “RFID: A Technical Overview and its Application to the Enterprise,” IEEE Computer Society, 2005

[3] G. De Vita , G. Iannaccone, “Design Criteria for the RF Section of Long Range Passive WID Systems,” IEEE Trans. *Microwave Theory and Techniques*, Vol.53, September 2005

[4] Jong-Wook Lee, Hongil Kwon, and Bomson Lee, “Design Consideration of UHF RFID Tag for Increased Reading Range,” IEEE MTT-S International, *Microwave Symposium Digest,* June 2006

[5] Joshua D. Griffin, Gregory D. Durgin, “Gains For RF Tags Using Multiple Antennas,“ *IEEE Transactions On Antennas and Propagation*, Vol. 56, No. 2, February 2008

[6] Leena Ukkonen, Lauri Sydänheimo, Markku Kivikoski, “Read Range Performance Comparison of Compact Reader Antennas for a Handheld UHF RFID Reader,” *IEEE International Conference on RFID 2007*

[7] G.A. Deschamps, "Microstrip microwave antennas," presented at the 3d USAF Symposium on Antennas, 1953.

[8] J.Q. Howell, "Microstrip antennas," IEEE APS Int. Symposium. Digest, pp. 1 77-1 80, 1972.

[9] R.E. Munson, "Conformal microstrip antennas and microstrip phased arrays," IEEE Trans. Antennas Propagation, Vol. AP-22, pp. 74-78, 1974.

[10] D. L. Rascoe, et al, ”Ka-band MMIC beam-steered transmitter array,” IEEE Trans. Microwave Theory & Techniques, vol. 37, pp. 2165-2168,Dec. 1989

[11] E. Levine, G. Malamud, and S. Shrikman, “A study of microstrip array antennas with the feed network,” IEEE Trans. Antennas Propagation, vol. 37, pp. 426–434, Apr. 1989.

[12] J.John Huang, “A technique for an array to generate circular polarization with linearly polarized elements,” IEEE Trans. Antennas Propagation, vol. AP-34, pp. 1113–1124, Sept. 1986.

[13] Hall, P.S.. Dahele. J.S., and James, J.R.: 'Design principles of sequentially fed, wide bandwidth. circularly polarized microstrip antennas," IEEE Proc. H, 1989, 136, pp. 381-389

[14] J. Bahl and P. Bhartia, "Microstrip antennas," Artech House Inc., Dehdam, Massachusetts, 1980.

[15] Y.T. Lo, D. Solomon, and W.F. Richards, "Theory and experiment on microstrip antennas," IEEE Trans. on Antennas and Propagation, Vol. AP-27, pp. 137-145, 1979.

[16] W.F. x”, Y.T. Lo and D.D. Harrison, "An improved theory for microstrip antennas and applications," IEEE Trans. on Antennas and Propagation, Vol. AP-29, pp. 38-46, 1981.

[17] J.R. Mosig, “Arbitrary shaped microstrip structures and their analysis with a mixed potential integral equation,” IEEE Trans. Microwave Theory Tech., Vol. 36, pp. 314-323, Feb. 1988.

[18] A. Hoorfar and V.Jamnejad, “Electromagnetic modeling and analysis of wireless communication antennas,” IEEE Microwave Magazine, Vol. 4, Iss.1, pp. 51- 67, Mar. 2003.

[19] Http://eesof.tm.agilent.com/products/momentum_main.html

[20] James J. R. & Hall P. S., Handbook of Microstrip Antennas, Peter Peregrinus Ltd.,1989

[21] Balanis C. A., Antenna Theory Analysis And Design, John Wiley & Sons Inc., 2nd ed., 1997.

[22] Carver K. R. & Mink J. W., Microstrip Antenna Technology, IEEE Trans. Antennas and Propagation, vol. 29, no. 1, pp 2-24, Jan. 1981.

[23] Inder J. Bahl, Prakash Bhartia, Stanislaw S. Stuchly, “ Design of Microstrip Antennas Covered with a Dielectric Layer,” IEEE Trans. Antennas and Propagation, vol. AP-30, no.2, pp. 314-318, March 1982.

[24] W. L. Stutzman and G. A. Thiele, Antenna Theory and Design. New York: John Wiley & Sons, Inc., 1998.

[25] D. R. Jackson and N. G. Alexopoulos, “Simple approximate formulas for input resistance, bandwidth, and efficiency of a resonant rectangular patch,” IEEE Transaction on Antennas & Propagation, vol. 39, no. 3, pp. 407–410, 1991.

[26] E. Chang, S. A. Long and W. F. Richards, “Experimental investigation of electrically thick rectangular microstrip antenna,” IEEE Trans. Antennas and Propagation, vol. AP-34, pp. 767-772, June 1986

[27] D. H. Schaubert, D. M. Pozar, and A. Adrian, “Effect of microstrip antenna substrate thickness and permittivity: comparison of theories and experiment,” IEEE Trans. Antennas and Propagation, vol. AP-37, pp. 677-682, June 1989.

[28] D. M. Pozar and D. H. Schaubert, “Scan blindness in infinite phased arrays of printed dipoles,” IEEE Trans. Antennas and Propagation, vol. AP-32, pp. 602-610, June 1984

[29] D. M. Pozar and D. H. Schaubert, “Analysis of an infinite array of rectangular microstrip patches with idealized probe feeds,” IEEE Trans. Antennas and Propagation, vol. AP-32, pp. 1101-1107, Oct. 1984

[30] J.P. Da**n**iel, G. Dubost, Terret, C. Citerne, J. Drissi, M.,” Research on planar antennas and arrays: `structures Rayonnantes,” IEEE Trans. on Antennas and Propagation, Vol. AP-35, pp. 14-38, Feb 1993

[31] J. Huang. ,” Dual-polarized microstrip array with high isolation and low cross-polarization,” Microwave and Optical Technology Letters, vol. 4, Feb. 1991, p. 99-103, 1991.

[32] T. Chiba, Y. Suzuki and N. Miyano, “Suppression of higher modes and cross polarized component for microstrip antennas,” IEEE Trans. on Antennas and Propagation, pp. 285-288, 1982

[33] D. M. Pozar and D. H. Schaubert, “Microstrip Antennas: The Analysis and Design of Microstrip Antennas and Arrays,” Wiley-IEEE Press Home, 1995

[34] RFID system. Available at http://www.alientechnology.com

[35] Waterhouse, R. B. (Rodney B.), “Microstrip patch antennas: a designer's guide,” Kluwer Academic Publishers, 2003

[36] Cheype, C.; Serier, C.; Thevenot, M.; Monediere, T.; Reineix, A.; Jecko, B , “An electromagnetic bandgap resonator antenna,” IEEE Trans. Antennas and Propagation, vol. AP-50, pp. 1285-1290, Sept 2002

[37] Egashira, S.; Nishiyama, E, “Stacked microstrip antenna with wide bandwidth and high gain,” IEEE Trans. Antennas and Propagation, vol. AP-44, pp. 1533-1534, Nov 1996

[38] K. J. Vinoy, K. A. Jose, V. K. Varadan, V. V. Varadan, “Gain-enhanced electronically tunable microstrip patch antenna,” Microwave and Optical Technology Letters, Volume 23 Issue 6, Pages 368 - 370

[39] A. P. Feresidis, G. Goussetis, S. Wang, and J. (Yiannis) C. Vardaxoglou, “Artificial Magnetic Conductor Surfaces and Their Application to Low-Profile High-Gain Planar Antennas,” IEEE Trans. Antennas and Propagation, vol. AP-53, January 2005

[40] Rahman, A.A.; Verma, A.K.; Omar, A.S., “High gain wideband compact microstrip antenna with quasi-planar surface mount horn,” IEEE MTT-S International, *Microwave Symposium Digest,* pp.571-574, June 2003